ARTICLE TYPE

Research Paper

TITLE

Interpreting vegetation change in tropical arid ecosystems from sediment molecular fossils and their stable isotope compositions: A baseline study from the Pilbara region of northwest Australia

AUTHORS

Alexandra Rouillard[11*], Paul F Greenwood[1-3], Kliti Grice[3], Grzegorz Skrzypek[1], Shawan Dogramaci[4], Chris Turney[5], Pauline F Grierson[1]

1. West Australian Biogeochemistry Centre and Ecosystems Research Group, School of Plant Biology, The University of Western Australia (UWA), Crawley WA, Australia.
2. Centre for Exploration Targeting, School of Earth and Environment, UWA.
3. Western Australia Organic and Isotope Geochemistry Centre; and John de Laeter Centre, The Institute for Geoscience Research, Department of Chemistry, Curtin University, Perth WA, Australia
4. Rio Tinto Iron Ore, Perth WA, Australia.
5. Climate Change Research Centre, University of NSW, Sydney NSW, Australia.

* Corresponding author: e-mail: alexandra.rouillard@snm.ku.dk; alexandrarouillard@yahoo.ca

[1] Present address: Centre for GeoGenetics, The Natural History Museum of Denmark, Øster Voldgade 5-7, 1350 Copenhagen K, Denmark

HIGHLIGHTS (max 85 characters)

- Biomarkers and *n*-alkane $\delta^{13}C$ were extracted from sediment with total C = 0.4–1.4%
- Distribution of biomarkers reflected a decrease of aridity in the last ~2000 years
- Arid based Bayesian model of *n*-alkanes $\delta^{13}C$ suggested increase of riparian C_3 input
- Provided interpretive framework for reconstructions in tropical arid ecosystems

KEY WORDS

Biomarkers; CSIA $\delta^{13}C$; *n*-alkanes; organic matter; Pilbara; *Triodia*

ABSTRACT

Detection of source diagnostic molecular fossils (biomarkers) within sediments can provide valuable insights into the vegetation and climates of past environments. However, hot and arid regions offer particularly challenging interpretive frameworks for reconstructing past conditions because baseline data are scarce, sedimentary organic matter contents are generally very low and in the inland tropics in particular, sediments are also often subject to periods of flooding and drought. However, there have been relatively few assessments of whether it is possible for biomarkers to be extracted in sufficient quantities from arid sediments to allow interpretation of past changes in vegetation and climate. Here, we measured the amounts, molecular distribution and $\delta^{13}C$ values of organic compounds extracted from a multi-dated (^{210}Pb, ^{137}Cs and ^{14}C) late Holocene sediment record from the Fortescue Marsh (Pilbara, northwest Australia) to investigate catchment vegetation history in relation to hydroclimatic change over recent millennia. The low total carbon (TC) content (<1.4 %) was a major challenge for the molecular analyses over the ~2000 years old sequence. Nevertheless, they revealed that the dominant hydrocarbon features (e.g., long chain *n*-alkanes) indicative of terrestrial plants (e.g., C_4 grasses; riparian and other C_3 plants) encompassed the last ~1300 yrs and that low abundance of products from aquatic sources (e.g., *n*-C_{17}) were detected in the uppermost sediments only when permanently inundated conditions prevailed (recent decades). Similarly, the lower $\delta^{13}C$ values (i.e., a difference of -2.3 ‰) of long chain *n*-alkanes in upper sediments reflected a vegetation response to the emergence of wetter conditions through the late Holocene in the region. Based on the diverging dominant source contributions obtained from the molecular distributions and arid based Bayesian mixing model ($\delta^{13}C$ of *n*-$C_{27\text{-}33}$ alkanes) results, less arid conditions may have favoured the input of ^{13}C depleted *n*-alkanes from the *Eucalyptus* (C_3) dominant riparian vegetation. The deepest sediments (<CE 700) however, had a TC content of <0.4 %, and no organic compounds were detected, consistent with local and regional records of hyperarid conditions. These results demonstrate that

57 *n*-alkanes can provide a molecular and stable isotopic fingerprint of important - and perhaps
58 underappreciated - ecological processes in modern tropical arid environments for future
59 paleoclimate investigations.

ABBREVIATIONS

CE	Common Era
CPI	Carbon preference index
CSIA	Compound-specific stable isotope analysis
GC-MS	Gas chromatography-Mass spectrometry
IRMS	Isotope ratio mass spectrometry
OM	Organic matter
TC	Total carbon

1. INTRODUCTION

Lake sediment records can extend temporal scales of hydrologic reconstruction to millennial and longer time frames. For example, periods of drought can be reconstructed from changes in lake level and salinity using microfossil assemblages (e.g., diatoms) and geochemical or physical parameters of the sediment (e.g., Wolff et al. 2011; Barr et al. 2014). These paleolimnological methods have most commonly been applied to closed-basin lakes in arid or semiarid landscapes, in which changes in lake level and salinity are closely related to shifts in hydrologic balance (e.g., Stager et al. 2013). However, deep or permanent lakes are often lacking in many arid environments, resulting in limited applicability of many proxies due to preservation issues, notably for reconstructing inputs of organic matter to lakes that can reflect hydroclimate conditions. Organic geochemical studies of depositional environments have provided molecular evidence (biomarkers) of changing hydrology under various climates, including from the studies of lakes (Leng and Henderson 2013; Sun et al. 2013; Atahan et al., 2015), marine settings (e.g., Castañeda et al. 2009b; Dubois et al. 2014; Pagès et al. 2014), and coastal salt-marshes and lagoons (e.g.,

85 Volkman et al. 2007; McKirdy et al. 2010; Tulipani et al., 2014). The sedimentary distribution of
86 biomarkers and their stable carbon and hydrogen isotope compositions (i.e., $\delta^{13}C$ and $\delta^{2}H$ at
87 compound specific level) have been widely used to investigate physiological or ecological
88 community responses to shifts in lake salinity and water source (Romero-Viana et al. 2012; Sachse
89 et al. 2012; van Soelen et al. 2013). Variation in the $\delta^{13}C$ values of specific compounds, e.g., long
90 chain *n*-alkanes representative of terrestrial vegetation, have also indirectly helped resolve past
91 hydrological changes via their sensitivity to moisture availability in the catchment, drought stress
92 or vegetation shifts (Castañeda et al. 2007; 2009a; Kristen et al. 2010; Tipple and Pagani 2010; Sun
93 et al. 2013). Consequently, using biomarkers and their stable isotopes ratios to establish
94 paleoenvironmental records for still underrepresented regions is of great interest.
95
96 Tropical arid ecosystems have proved especially challenging to paleolimnology and organic
97 geochemical characterisation of sediments. These regions experience high seasonal and inter-
98 annual hydroclimatic variability, typified by periods of prolonged droughts interspersed with
99 occasional intense flooding (e.g., Rouillard et al. 2015; van Etten 2009). First, a general lack of
100 water, which is often coupled with low nutrient availability, severely limits biological production
101 and in turn the deposition of organic matter (OM) to sediments (e.g, Huxman et al. 2004; Snyder
102 and Tartowski 2006; Collins et al. 2008; McIntyre et al. 2009a, b). In Australian soils of tropical (i.e.,
103 hot) arid environments in particular, the preservation of OM is further compromised by major
104 biological reworking by termites and other fauna (e.g., Holt et al. 1987; Chen et al. 2003; Austin et
105 al. 2004) and the high frequency of fires which can accelerate the loss of organic volatiles that
106 might otherwise form terrestrial detritus (Ford et al. 2007). Intense episodic flooding can lead to
107 increased mobilisation and dislocation of OM from the catchment to lakes followed by pulses of
108 high organic production in the catchment and aquatic network, resulting in non-linear OM
109 availability and deposition patterns (Battin et al. 2008; Reid et al. 2011; Puttock et al. 2012).

110 Shallow lakes mean that prolonged drought further exposes dried sediment to changing redox
111 conditions and deflation, which can also cause hiatus of organic sedimentary records in many
112 regions of the world (Verschuren et al. 1999; Bessems et al. 2008; Argus et al. 2014, 2015). Given
113 these challenges, there have been few attempts to characterise such sediments in northwest
114 Australia, a region where very limited knowledge of the Holocene environmental history is
115 available to understand long-term ecosystem processes and resilience to ongoing climate change
116 (Gergis et al. 2014).
117
118 Plant molecular δ^2H signals are normally considered indicative of the isotope ratio of source water
119 and associated hydrology (Tipple and Pagani 2010; Romero-Viana et al. 2012; Sachse et al. 2012;
120 van Soelen et al. 2013). However, the large evaporative shifts in lake volumes in arid and semi-arid
121 regions generally result in salinity fluctuations that in turn affect the δ^2H fractionation between
122 organisms and their source water (Sachse and Sachs 2008). In addition, plants make physiological
123 adjustments to both changing water availability and salinity, which can also result in further
124 fractionation (Zhou et al. 2011; Sachse et al. 2012), making plant molecular δ^2H less reliable than
125 in more temperate or non-saline ecosystems (e.g., Duan et al., 2014). Consequently, plant
126 molecular δ^{13}C compositions of sediments, particularly of *n*-alkanes, may be more suitable for hot
127 arid environments.
128
129 The composition and distribution of plant communities in arid ecosystems is largely driven by the
130 availability of water as well as other flooding or waterlogging-related conditions, such as soil
131 redox, salinity, substrate and nutrient availability and the accumulation of toxic ions (Schwinning
132 et al. 2004; Reid et al. 2011; Argus et al. 2014). Different hydrological regimes will favour plants of
133 specific functional types (e.g., C_3 versus C_4 photosynthetic pathways, which are readily
134 distinguished by their δ^{13}C signatures) and tolerance to drought, waterlogging or salinity (Huxman

et al. 2004; Snyder and Tartowski 2006). Prolonged aridity can thus progressively impact vegetation assemblages at the generation level over long timescales, generally favouring C_4 grasses across catchments and chenopods (often a mix of CAM, C_4 and C_3 species) in saline wetland areas (Sage et al. 2011). The ^{13}C enrichment of C_3 plant tissue can also be driven by water stress within a matter of minutes (Cernusak et al. 2013). The dynamics of plant water stress over periods of decades to centuries may also be recorded in the wood chemistry of trees (e.g., Cullen et al. 2008; Qin et al. 2015) or at the ecosystem level in soils and lake sediment (Krull et al. 2005, 2006; Diefendorf et al. 2011; Codron et al. 2013). Plants in arid environments also produce relatively high amounts of cuticular waxes as a protection against high ultraviolet light and water loss; cuticular waxes may thus represent more promising molecular targets of organic lean dryland sediments (Hoffmann et al. 2013).

Cuticular-derived *n*-alkanes (Eglinton and Hamilton 1967) are typically some of the more abundant products from the organic sediments of lakes (Schmidt et al. 2011), so are attractive analytes for compound specific isotopic analysis (CSIA). Characterisation of the molecular and stable isotopic abundances of *n*-alkanes has become an important paleoecological strategy to assess changes in hydrological status at catchment and continent scales (Castañeda and Schouten 2011; Sachse et al. 2012; Leng and Henderson 2013; Dubois et al. 2014). In recent years, the $\delta^{13}C$ values of *n*-alkanes in sediments have unlocked a wealth of paleoenvironmental information from regions and sites that had previously been difficult, including assessment of historical change in catchment land-use, eutrophication studies and shifts in vegetation composition in response to climate (e.g., Castañeda and Schouten 2011; Fang et al. 2014). However, as with other relatively new molecular tools in paleolimnology, our capacity to make inferences of paleo-flora from biomarkers is limited by uncertainties in source, transportation and preservation of OM from senescing plants (Birks and Birks 2016). A first step is to improve the baseline of available biomarker datasets and their

160 stable isotopic compositions from arid zone sediments with independently described
161 paleoenvironmental histories.
162
163 Broadly, our study investigated the potential of organic molecular fossils and $\delta^{13}C$ values of plant
164 waxes of lake sediments for reconstructing catchment vegetation history and hydroclimatic
165 change in the arid subtropical Pilbara region of inland northwest Australia. Previously, we
166 established centennial and millennial flood records for the Pilbara based on historical records as
167 well as physical and geochemical analyses of sediments at the Fortescue Marsh (Rouillard et al.
168 2015; Rouillard et al. 2016). Here, we used a replicate core of this sediment sequence to
169 determine if: i) organic geochemical information can be extracted to identify the major sources of
170 sedimentary OM; ii) $\delta^{13}C$ values of *n*-alkanes reflect the major vegetation types in the catchment
171 (C_3 and C_4); and iii) the molecular fossils and their $\delta^{13}C$ values from sedimentary OM can be related
172 to change in hydrology through the late Holocene in the region. Our analysis is considered within
173 an interpretive framework that accounts for the specificities and challenges of extracting
174 palaeoclimate information from organic geochemical indicators in sediments developed in tropical
175 arid ecosystems.
176
177 **2. METHODS**
178 **2.1 Study site**
179 The study region and sampling is described in detail in Rouillard et al. (2016 in review). Briefly,
180 replicated ~60-cm sediment cores (FOR106C2 and FOR106C3) were obtained from the deepest
181 section of the 14 Mile Pool (22.6˚S, 119.9˚E) of the Fortescue Marsh in the arid Pilbara region of
182 northwest Australia (Fig. 1). The pool is the most perennial water feature of the Fortescue Marsh,
183 which acts as a terminal lake for the Upper Fortescue River catchment (31,000 km^2) (Skrzypek et.
184 al. 2013). The Pilbara experiences highly episodic large hydrological events with high inter-annual

variability, i.e., creeks and rivers are generally dry with seasonal floods commonly occurring during the austral summer contributing brief periods of high flow (www.water.wa.gov.au). Evaporation is high in the eastern Pilbara (~2800–3200 $mm \cdot yr^{-1}$) and greatly exceeds average rainfall (290 $mm \cdot yr^{-1}$; www.bom.gov.au/climate/data). Flooding, drought and fire are the dominant and naturally occurring ecological disturbances in the region (McKenzie et al. 2009); variability in the seasonal and inter-annual hydrological cycle is extreme (Kennard et al. 2010; Rouillard et al. 2015) and likely influences the fire regime through feedback interactions (e.g., O'Donnell et al. 2011).

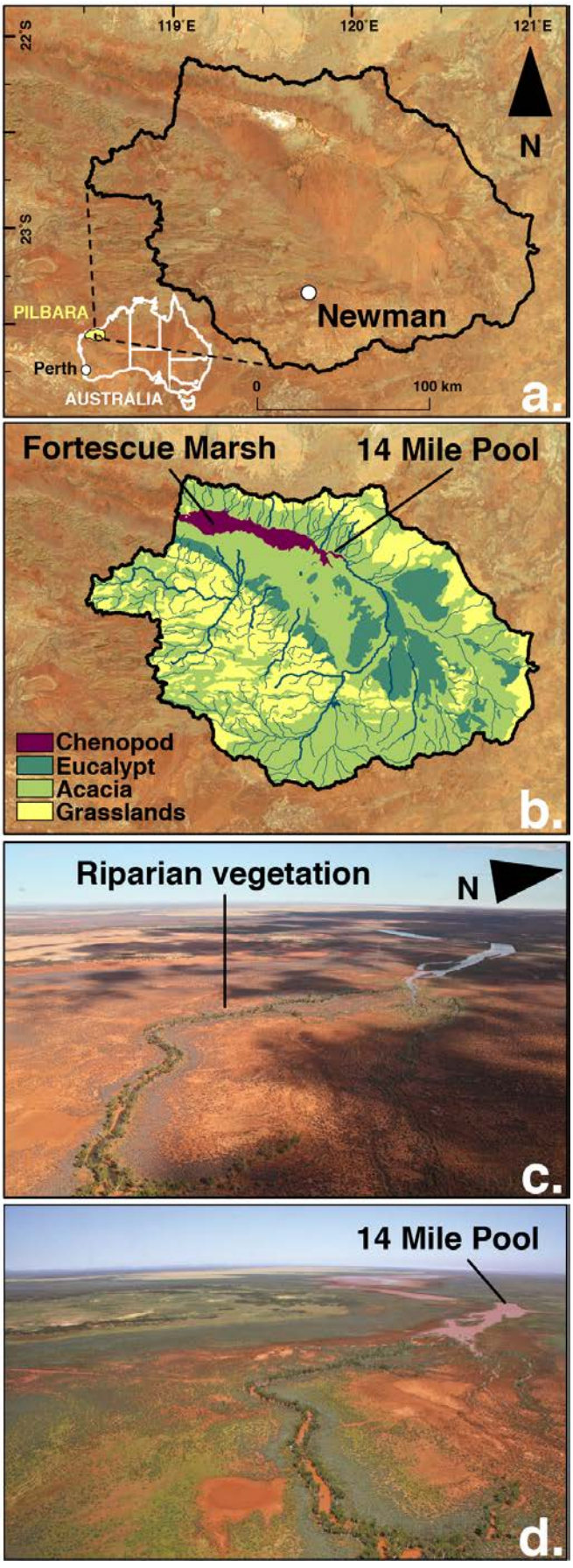
119°E
120°E
121°E
22°S
23°S
N
Newman
PILBARA
Perth
AUSTRALIA
0
100 km
a.
Fortescue Marsh
14 Mile Pool
Chenopod
Eucalypt
Acacia
Grasslands
b.
Riparian vegetation
N
c.
14 Mile Pool
d.

192

193

194 **Figure 1: a–b)** Upper Fortescue River catchment delineated (solid black line) on a True-colour
195 Aqua MODIS image (5, Jan 2005; NASA 2005), including b) a vegetation map with Chenopod
196 (Shrublands, Sampire Shrubland and Forblands), Eucalypt (Woodlands; Open Woodlands), Acacia
197 (Shrublands; Open Woodlands; Forests and Woodlands) and Grasslands (Hummock (*Triodia* spp);
198 Tussock); and **c–d)** aerial photographs (flowing East–West, the Upper Fortescue River, the 14 Mile
199 Pool and the Fortescue Marsh) of the **c)** riparian vegetation remaining (green) during dry
200 conditions (Jul, 2010; Photograph: Clive Taylor) and **d)** the greening effect of large rains during the
201 wet season (Feb 2012, one month after Severe Tropical Cyclone Heidi).
202 (1-COLUMN FITTING IMAGE)
203
204 Vegetation across the hills and broad plains of the wider catchment is mainly shrub-steppe,
205 dominated by C_4 grasses, especially spinifex (*Triodia* spp.) grasses and *Acacia* trees and shrubs (C_3).
206 More permanent watercourses, including 14 Mile Pool, maintain a riparian fringe dominated by
207 the trees *Eucalyptus camaldulensis* and *E. victrix* (C_3) (Fig. 1b, d; Beard 1975). Buffel grass
208 (*Cenchrus ciliaris*—C_4) is an invasive perennial grass introduced in the 1920s that was also aerial
209 seeded across the catchment in the 1960s to provide higher quality feed for cattle and sheep
210 grazing; this grass is abundant in the floodplains of sections of the Upper Fortescue River
211 (McKenzie et al. 2009). The Marsh downstream from 14 Mile Pool is dominated by chenopod
212 shrubs, primarily *Tecticornia* species (Beard 1975) that have been attributed both C_3 and C_4
213 pathways (Carolin et al. 1982; Voznesenskaya et al. 2008; Moir-Barnetson 2014).
214
215 **2.2 Analyses**
216 *2.2.1 Abundance and bulk stable isotopic values of total and organic sedimentary carbon*
217 As per reported in Rouillard et al. (2016), relative abundance (%) and stable isotope composition
218 (‰) of the sediment total C, organic C and total N were determined for every other interval (1 cm)

of core FOR106C3 using a Thermo Flush Elemental Analyser coupled with a Delta V Plus Isotope Ratio Mass Spectrometer (Thermo Fisher Scientific, Bremen, Germany). Stable isotope results are reported in permil (‰) after multi-point normalisation to international Vienna Pee Dee Belemnite standard (VPDB) scale using international reference materials NBS19, USGS24, NBS30, LSVEC (Skrzypek 2013), with combined analytical uncertainty <0.10 ‰. All samples were freeze-dried, ground using mortar and pestle and homogenised prior to analyses. To isolate the organic fraction, approximately 100–150 mg of ground sample was treated with 4 % HCl at room temperature overnight to remove carbonates prior to analysis. Acid pre-treatment for the removal of inorganic carbon (IC) can lead to biases beyond instrumental precision in C abundance and $\delta^{13}C$ measurements (e.g., 4 ‰; Brodie et al. 2011), which may become particularly significant when total C-content is very low, as is the case with these Pilbara sediments (Table 2). The total C and $\delta^{13}C$ results are therefore reported for total C without any acid pre-treatement i.e., without prior removal of inorganic C in the sediments.

2.2.2 Extraction and isolation of lipids

The sediment record of Fortescue Marsh at 14 Mile Pool comprises four distinct stratigraphic periods, together spanning several millennia of the marsh's environmental history (Rouillard et al. 2016). Replicate core FOR106C2 was separated into four sections each corresponding to one of the four periods, which were then each ground using mortar and pestle, homogenised and analysed for their molecular and stable carbon isotopic composition. Briefly, the sections and ages of the four periods we investigated and described in Rouillard et al. (2016) corresponded to Period 1 (P1; 1–19 cm, CE 1990–2012); Period 2 (P2; 19–40 cm, CE 1600–1990); Period 3 (P3; 40–49 cm, CE 700–1600) and 4 (P4; 49–61 cm, CE <100–700). Several dating methods (^{210}Pb, ^{137}Cs and ^{14}C) have coherently estimated the age of the record to encompass the last ~2000 years. Details of the dating procedures for the sediment record based on both replicates (FOR106C2 and FOR106C3)

and hydrological interpretations based on the analysis of lithology, moisture content, particle size, microfossils, total C and N content and total stable isotope compositions (δ^{13}C and δ^{15}N) on replicate core FOR106C3 exclusively have been previously reported (Rouillard et al. 2016). To summarise the hydrological interpretations, near perennial aquatic conditions were inferred for P1; P2 sediments reflected a relatively drier and highly variable environment than P1 with episodic extreme flood disturbance; P3 and P4 both reflected generally more arid conditions than P1 and P2 and low energy hydrologies; conditions from the base of the record in P4 were likely hyperarid until relatively less arid conditions and more regular flooding established during P3 from ~CE 700 (Rouillard et al. 2016). Unfortunately, concentrations of pollen grains in the sequence were very low and high levels of deterioration were evident, likely reflecting the rewetting and subsequent drying of the sediment cracking clays (Cushing, 1967; Lowe, 1982). Therefore, pollen could not be used as a reliable indicator of past vegetation at this site (Rouillard et al. 2016).

The four samples (~20 g) from the FOR106C2 core were separately extracted in a Soxhlet apparatus using a mixture of dichloromethane (DCM) and methanol (90:10, v/v) for 48-hr. Elemental sulfur was removed through the extraction by the prior addition of activated copper turnings to the sample (Blumer 1957). The total solvent-extracted bitumen was separated by small column chromatography (activated silica stationary phase 150˚C, 8h; 4 cm Pasteur pipette) into saturate, aromatic and polar hydrocarbon fractions by successive elution with 2 mL *n*-hexane, 2 mL *n*-hexane:DCM (3:1) and 2 mL DCM:methanol (1:1) (Pagès et al. 2015). Fraction yields were quantified but with relatively high uncertainty because of the very low masses extracted (total extractable fraction <160 $\mu g \cdot g^{-1}$ dry sediment).

2.2.3 Gas chromatography - mass spectrometry (GC-MS) analysis of hydrocarbon fractions

GC-MS of the aliphatic and aromatic hydrocarbon fractions was conducted with an Agilent 6890 GC interfaced to a 5973 mass selective detector (MSD). The GC was fitted with a 60-m capillary column (HP 5MS, cross-linked 5 % phenyl 95 % methyl-polysiloxane, 0.25 mm i.d., 0.25 µm film thickness), used He carrier gas (1.1 $mL \cdot min^{-1}$) and analyses were conducted in pulsed splitless mode with the injector at 280˚C. Full scan (*m/z* 50–550) 70 eV mass spectra were acquired, with product assignments based on GC retention time or mass spectral correlation with the Wiley275 MS library, other laboratory standards or published data. Peak areas in the total ion chromatogram (TIC) were used for quantification, except for steroids and terpenoids whose peak areas were measured from *m/z* 217 and *m/z* 191 fragmentograms, respectively. Only products detected at > 1 % the total TIC or fragmentogram signals were used for quantification.

The P_{aq} index was calculated for each sediment period. P_{aq} is defined as:

$$(n\text{-}C_{23} + n\text{-}C_{25})/(n\text{-}C_{23} + n\text{-}C_{25} + n\text{-}C_{29} + n\text{-}C_{31})$$

and has been used previously as a proxy for the relative contributions of algal, macrophytic and terrestrial inputs in lacustrine environments (Ficken et al. 2000). In individual plants, P_{aq} values of >0.4 are consistent with mainly algal input; 0.1–0.4 indicates a mainly macrophytic source and <0.1 implies a mainly terrestrial origin.

2.2.4 Compound-specific $\delta^{13}C$ analyses

Compound-specific stable carbon isotope compositions were measured with an Agilent 6890 GC coupled with a Micromass IsoPrime2 isotope ratio mass spectrometer (IRMS). The GC instrument was fitted with a 60 m length, 0.25 mm i.d., 0.25 µm thick DB-1 phase column and analyses were conducted in pulsed splitless mode following setup as in Pagès et al. (2015). Stable carbon isotope compositions (‰), determined by integration of the m/z 44, 45 and 46 ion currents of the CO_2 peaks from each compound, were reported in the delta notation ($\delta^{13}C$) all reported values are averages of at least triplicate analyses (standard deviation ≤0.2 ‰). The precision and accuracy of

293 the isotopic measurements were maintained by multi-point normalisation using the linear
294 regression slope and intercept obtained from frequent measurements (*n*=38; average standard
295 deviation = 0.2 ‰) of an in-house standard mixture of *n*-alkanes (*n*-$C_{14,}$ -$C_{17,}$ -$C_{19,}$ and -C_{25}) of
296 known isotopic composition (respectively: -30.99, -29.72, -32.12, -31.94 ‰). Raw $\delta^{13}C$ values were
297 recalculated to VPDB scale using multipoint normalisation based on an in-house standard mixture
298 of four *n*-alkanes (*n*-C_{14}, -C_{17}, -C_{19}, and -C_{25}) of known isotopic composition (respectively: -30.99, -
299 29.72, -32.12, -31.94 ‰ VPDB). Analytical precision of the stable isotope measurements were
300 monitored by frequent measurements of laboratory standards (*n*=38), including the additional *n*-
301 C_{11}, *n*-C_{13}, and *n*-C_{18} (respectively: -26.0; -29.3; -30.6 ‰ VPDB), during samples analyses and it was
302 ≤0.2 ‰ (one standard deviation).
303
304 *2.2.5 Mixing model to determine sources of* n-*alkanes*
305 Probability estimates of the proportional contribution of terrestrial C_3 versus C_4 arid plants to the
306 $\delta^{13}C$ values of the long-chain odd *n*-alkanes (*n*-C_{27} to *n*-C_{33}) were obtained using the Bayesian
307 isotopic mixing model of the SIAR package (Parnell et al. 2010) in R v. 3.1.1 (MCMC = 30000). Two
308 source end-members in the mixing model were based on a subset of leaf wax $\delta^{13}C$ values from C_3
309 and C_4 plants exclusively from arid regions and with taxonomic relevance to the Upper Fortescue
310 River catchment (summarised in Table 1) to account foliar $\delta^{13}C$ differences caused by water stress
311 (Weiguo et al. 2005; Diefendorf et al. 2010; Kohn 2010; Schulze et al. 2014) and other adaptive
312 differences among species (e.g., Turner et al. 2008). Owing to the paucity of published data for
313 arid Australia, the source dataset included a subset of 50 species mainly from southern African
314 savannas. Published records of *n*-alkane $\delta^{13}C$ values (331 entries; 280 species) were restricted to
315 taxa (mainly Genera, but also Family) found in the eastern Pilbara (*FloraBase*;
316 www.florabase.dpaw.wa.gov.au).
317

318

Table 1: Relative abundances of *n*-alkanes (% odd *n*-$C_{27–33}$) and their stable isotopic signatures ($\delta^{13}C$) in leaves from C_3 and C_4 plant taxa found in the semi-arid Pilbara (Arid) and in various climates (All). Sources: Collister et al. 1994; Ficken et al. 2000; Chikaraishi and Naraoka 2003; Bi et al. 2005; Mead et al. 2005; Krull et al. 2006; Rommerskirchen et al. 2006; Tanner et al. 2007; Pedentchouk et al. 2008; Vogts et al. 2009; Diefendorf et al. 2010; Kristen et al. 2010; Tanner et al. 2010; Diefendorf et al. 2011.

		n-C_{27}	std	*n*-C_{29}	std	*n*-C_{31}	std	*n*-C_{33}	std	*n*	mean	std
Arid												
Abundance	C_3	21	± 14	36	± 19	30	± 14	13	± 15	20	25	± 15
	C_4	11	± 7	16	± 7	45	± 13	29	± 15	30	25	± 10
$\delta^{13}C$	C_3	−32.5	± 2.1	−33.3	± 1.8	−34.2	± 2.2	−35.2	± 1.9	8–22	−33.8	± 2.0
	C_4	−22.0	± 2.6	−21.9	± 2.0	−22.4	± 2.2	−22.3	± 1.8	30–32	−22.2	± 2.2
All												
Abundance	C_3	15	± 17	38	± 24	33	± 19	14	± 18	138	25	± 19
	C_4	14	± 12	18	± 12	39	± 15	29	± 18	49	25	± 14
$\delta^{13}C$	C_3	−32.4	± 2.8	−36.2	± 2.6	−33.7	± 3.1	−36.8	± 2.9	94–176	−34.7	± 2.9
	C_4	−23.2	± 5.1	−24.9	± 5.0	−23.6	± 5.1	−25.1	± 5.5	67–88	−24.2	± 5.2

(2-COLUMN FITTING TABLE)

Descriptive statistics of the arid zone C_3 and C_4 end-members used in the mixing model ($\delta^{13}C$ and abundance) were then compared with those of the full dataset incorporating non-Pilbara vegetation to validate subsequent interpretation. As would be expected, *n*-alkanes of the terrestrial C_3 (n = 22) and C_4 (n = 32) plants formed distinct groupings within the $\delta^{13}C$ data set with minimum overlap (Table 1). Briefly, *n*-alkanes of C_3 plants had significantly ($p<0.005$) lower $\delta^{13}C$ values than C_4 in both the arid exclusive (C_3=−33.8 ± 2.0 ‰; C_4=−22.2 ± 2.2 ‰) and the full plant datasets (C_3=−34.7 ± 2.9 ‰; C_4=−24.2 ± 5.2 ‰). The average $\delta^{13}C$ values for the *n*-alkanes of C_3 and C_4 plants were both slightly higher and had smaller standard deviations in the arid dataset than the full dataset; however, this difference was not significant ($p>0.1$). Based on the same subset, we used an abundance matrix (Table 1) of the selected *n*-alkanes relative to one another (%) to account for the effect of concentration-dependence biases on mixing model estimates (Phillips and Koch 2002). The average *n*-alkane abundances calculated for C_3 or C_4 sources from

the full datasets as well as the smaller subset of arid zone data were also consistently and significantly different (p-value<0.005), except for n-C_{27} (p=0.7) and n-C_{31} (p=0.06). In addition, n-$C_{27, 29}$ were more abundant in C_3 plants while n-$C_{31, 33}$ were more abundant in C_4 plants, and was most pronounced for arid species. However, there was no significant difference (p=0.06) in the relative abundance of the n-alkanes between the full and arid only datasets for either C_3 or C_4.

3. RESULTS

3.1 Organic matter composition

3.1.1 Bulk OC and solvent-extractable compounds

Sediment C and N abundances and stable isotope compositions are described in relation to each of the four hydroclimate periods described previously for this region: P1 (1–19 cm, CE 1990–2012), P2 (19–40 cm, CE 1600–1990), P3 (40–49 cm, CE 700–1600) and P4 (49–61 cm, CE <100–700). Total C was very low in all sediments (Table 2). TC content was highest in P1 (1.4 %) and lowest in P4 (< 0.4 %), with P2 (0.6 %) and P3 (0.7 %) between these values. Similarly, the highest N content as well as lowest δ^{15}N were found in P1 (0.12 % wt and 6.1 ‰). Conversely, the lowest N content and highest δ^{15}N were found in P4 (0.01 % wt and 7.6 ‰). P2-P3 showed similar intermediate values (0.03 % wt and 7.4-7.5 ‰). The total solvent-extractable bitumen fraction (Table 2) of P1–P3 was 60 to 150 $\mu g \cdot g^{-1}$ of sediment, representing around 1 % of total C. Polar compounds dominated the bitumen (NSO - nitrogen, sulfur and oxygen polar compounds - fraction >89 %), whereas the aliphatic fractions were between 2 and 5 % (P3>P1>P2) and the aromatic fraction even smaller in P1 and P3 (<1 %). The aromatic fraction of P2 was relatively high at 8.5 %. The extractable fraction (i.e., bitumen) of P4 sediment was <5 $\mu g \cdot g^{-1}$ of sediment, which was insufficient for further characterisation. Sediment δ^{13}C values for the entire core were in the range -20.3 to -28.2 ‰, which are typical values of biologically sourced sedimentary OM (e.g., with

mixed C_3/C_4 inputs) and imply negligible carbonate influence on measured $\delta^{13}C$ (Finlay and Kendall 2008).

Table 2: Geochemical parameters of four organic sedimentary periods (P1–P4) from the 14 Mile Pool sediment record, NW Australia.

Parameter			P1 (1990–2012[1])	P2 (1600–1990)	P3 (700–1600)	P4 (<100–700)	Total Av (<100–2012)
Bulk sediment content & stable isotopes	n (combined intervals)		17	23	7	11	58
	Total C (%wt)		1.4	0.6	0.7	<0.4	0.8
		Range	0.8–5.6	<0.4–1.1	0.5–0.9	<0.4–0.5	<0.4–5.6
	Total N (%wt)		0.12	0.03	0.03	0.01	0.05
		Range	0.06–0.17	0.01–0.06	0.02–0.03	<0.01–0.01	<0.01–0.17
	$\delta^{13}C$ [‰ VPDB]		−24.3	−22.9	−20.3	−28.2	−23.4
		Range	−26.7–−22.3	−26.2–−20.2	−22.4–−16.9	−28.4–−28.0	−28.4–−16.9
	$\delta^{15}N$ [‰ AIR]		6.1	7.5	7.4	7.6	7.1
		Range	4.8–8.4	6.5–7.9	7.0–7.6	7.5–7.8	4.8–8.4
Yield	Tot ext ($\mu g \cdot g^{-1}$)		155	87	63	< 5	-
	Aliphatic (% tot)		4.7	2.6	5.0	-	-
	Aromatic (% tot)		0.3	8.5	0.7	-	-
	NSO (% tot)		95	89	94	-	-
Aliphatic fraction	Alkanes (%TIC)		84	61	71	-	-
	Steroids (%TIC)		1.4	8.1	7.2	-	-
	Hopanoids (%TIC)		2.7	4.2	5.8	-	-
	Others (% TIC)		12	27	16	-	-
CPI	n-$C_{23–33}$		3.1	5.7	5.0	-	-
P_{aq}			0.3	0.1	0.3	-	-
Mixing	C_3 (%)		59	53	50	-	-
	C_4 (%)		41	47	50	-	-

Note: [1]All time periods are provided in years of the Common Era (CE); C and N content (Total C and Total N) and stable carbon and nitrogen isotopes ($\delta^{13}C$ and $\delta^{15}N$) (modified from Rouillard et al. 2016); estimated yields of the total extractable fraction (Tot ext; $\mu g \cdot g^{-1}$ of sediment); the aliphatic, aromatic and polar (NSO) fractions are expressed as a % of the total extractable fraction; relative abundance of *n*-alkanes, steroids, hopanoids and other aliphatic compounds on the total ions chromatogram (%TIC); carbon preference index (CPI) and P_{aq} index (see

(2-COLUMN FITTING TABLE)

3.1.2 Aliphatic hydrocarbon fractions

GC-MS analysis of the aromatic fractions yielded very few products; however, a wide distribution of aliphatic hydrocarbons were detected in the saturated fractions of P1–P3. The main aliphatic products included: *n*-alkanes, regular isoprenoids (e.g., phytane), branched alkanes and alkenes and saturated and unsaturated hopanoids and steroids. A particularly prominent homologous series of C_{17} to C_{35} *n*-alkanes accounted for ~60 to 85 % of the TIC signal of the saturate fraction, where n-C_{31} was the most dominant analyte (15–21 % of TIC; Fig. 2). The carbon preference index (CPI) was separately calculated for long-chain (C_{23} to C_{33}) *n*-alkanes (e.g., Bray and Evans 1961;

388 Kuhn et al. 2010; Rao et al. 2008). The longer chain members showed a strong odd-over-even
389 predominance ($CPI_{23–33}$ = 3–6; P2>P3>P1; Table 2). The P_{aq} values of P1–P3 were 0.1 or 0.3
390 suggesting the OM may mostly originate from macrophytes (Ficken et al. 2000). However, it is
391 important to note that the P_{aq} value in sediment extracts likely reflect a mixture of inputs and may
392 therefore also integrate a signal from both terrestrial and aquatic sources (Ficken et al. 2000). Less
393 abundant products across P1–P3 included a similar series of monounsaturated *n*-alkenes, as well
394 as several branched alkanes including the regular isoprenoids pristine and phytane and polycyclic
395 hopanoids and steroids. The hopanoids, best seen from the *m/z* 191 fragmentogram (Fig. 2 top),
396 included C_{27} to C_{31} hopanes and even more abundant mono- and diunsaturated hopenes ($hC_{28–30=}$),
397 tricyclic terpanes ($tC_{19–24}$) and the C_{24} tetracyclic terpane (TC_{24}). The steroids included C_{28} to C_{30}
398 steranes ($sC_{28–30}$) as well as several short chain steranes ($sC_{19–22}$). The distribution of aliphatic
399 products detected across sediment depths (P1–P3) were broadly similar. However, pristane and
400 phytane were only detected in P1. The P1 sediments also showed a greater diversity, but lowest
401 relative abundance, of hopanoid and steroid products. In contrast, *n*-alkenes were detected in P2
402 and P3 but not P1. Sediments of P2 had the highest representation of aliphatics other than *n*-
403 alkanes. These were mainly linear branched alkanes and alkenes; short chain steranes ($sC_{19–22}$)
404 were the major steroids of P1 (>50 % of *m/z* 217 steroid signal) while sterenes were particularly
405 high in P2 and P3 (>80 % of *m/z* 217; Fig. 3).
406

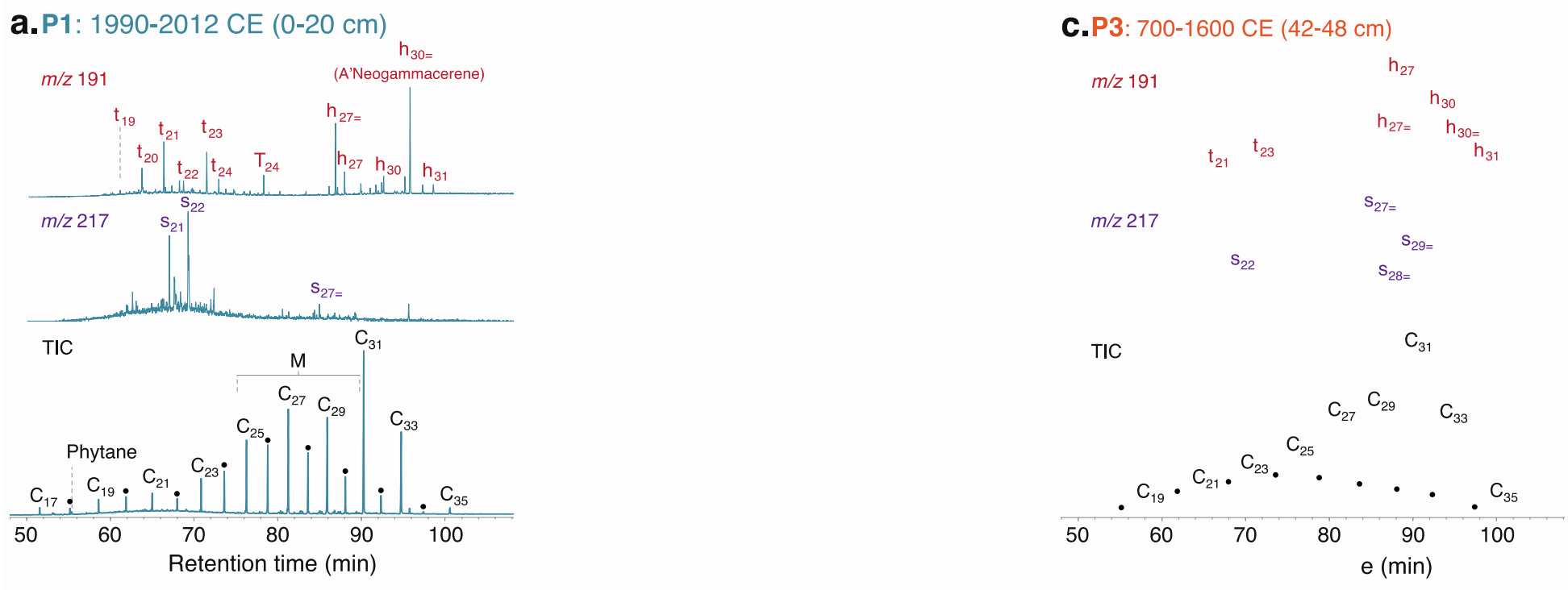

Figure 2: GC-MS total ion chromatograms (TIC) and fragmentograms (*m/z* 191 and 217) of the three periods in the core; (a) P1, (b) P2 and (c) P3. Tentatively assigned compounds are labelled with their corresponding carbon number and unsaturation level (=); odd (C) and even (filled circles) *n*-alkanes, tricyclic terpanes (t), tetracyclic terpanes (T), steroids (s), hopanoids (h) methylated alkane series range (M) and linear aliphatic series (open circles).

(1.5-COLUMN FITTING IMAGE)

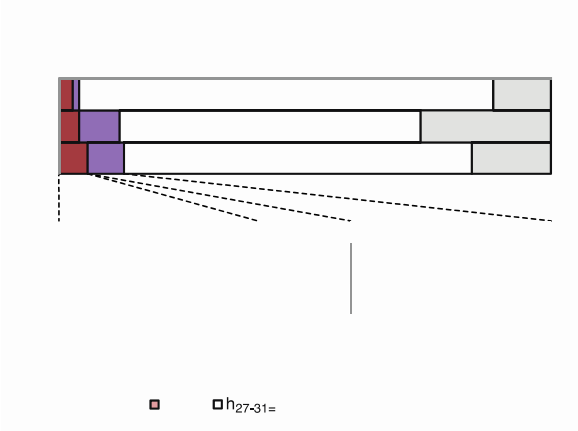

Figure 3: Relative peak abundances (% TIC) of the main aliphatic compounds extracted by GC-MS and quantitative distributions of hopanoids and steroids within each sedimentary period.

(1-COLUMN FITTING IMAGE)

3.1.3 $\delta^{13}C$ of n-*alkanes*

Stable carbon isotope values were measured for most *n*-alkanes detected in the P1–P3 samples (Table S1; Fig. 4). However, the concentrations of other aliphatic products were too low for accurate $\delta^{13}C$ measurement. The $\delta^{13}C$ value range for *n*-alkanes was mostly in a relatively narrow range (±2 ‰) around -29 ‰. Overall minimum $\delta^{13}C$ was −32.3 ± 0.1‰ (*n*-C_{17} in P1) and maximum $\delta^{13}C$ was −24.0 ‰ (*n*-C_{35} in P3). The $\delta^{13}C$ values of the mid-chain n-alkanes (*n*-$C_{21–26}$) were similar in P1 and P3, but higher by ~2 ‰ in P2. The odd n-alkanes had higher $\delta^{13}C$ values compared to their even carbon neighbours, particularly for the longer-chain compounds (>*n*-C_{27}) where this differential was as much as ~1‰ in sediments from for P2. The $\delta^{13}C$ values of the odd numbered *n*-alkanes from *n*-C_{27} followed the trend of P1<P2<P3 i.e., increasing with sediment depth and age (Fig. 4).

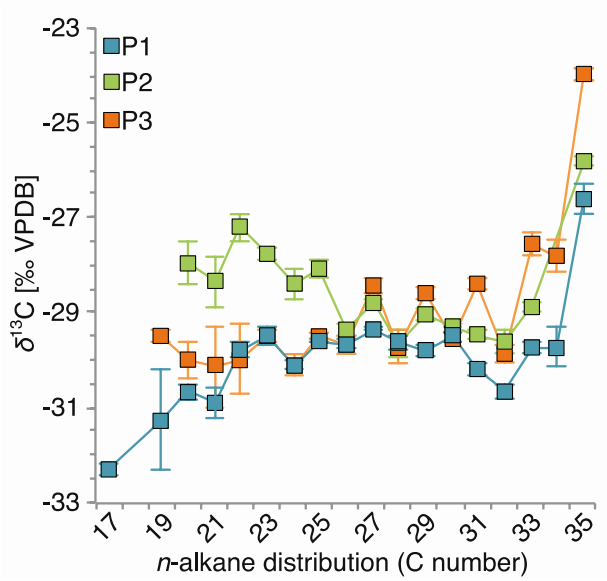

433

434

435 **Figure 4**: Average carbon stable isotopic signature ($\delta^{13}C$) of the *n*-alkanes extracted from each

436 sediment period: P1 (blue), P2 (green) and P3 (orange). Error bars represent the standard

437 deviation obtained from triplicate measurements.

438 (1-COLUMN FITTING IMAGE)

439

440 **3.2 Sources of organic matter based on mixing model of long-chained *n*-alkanes**

441 The mixing model based on $\delta^{13}C$ values of the long-chain odd *n*-alkanes (*n*-C_{27} to *n*-C_{33}) for P1–P3

442 is shown in Figure 5b. Typical of two-end member mixing models all probability distributions were

443 unimodal (Parnell et al. 2010; Hopkians and Ferguson 2012; Fig. 5). The model suggests terrestrial

444 C_3 dominance over recent decades (~20 years) (P1 median = 59 %; Table 2; Fig. 5), but with

445 increasing importance of C_4 OM sources in the sediments of P2 (C_3 median = 53 %) to co-

446 dominance of C_3 and C_4 sources in P3 (C_3 ~ C_4 = 50 %). The probability distributions for C_3 and C_4

447 are wide and overlapping indicating a high uncertainty with these estimates, however diverging

448 median values suggests an increasing C_3 contribution and corresponding decrease in the C_4 with

449 time (Fig. 5). While small aquatic and macrophytic inputs were detected in the molecular

450 distributions, their contributions are unlikely to weight significantly on the mixing model estimates

given the strong terrestrial plant signal of the abundant long-chain *n*-alkanes used here (see Discussion below).

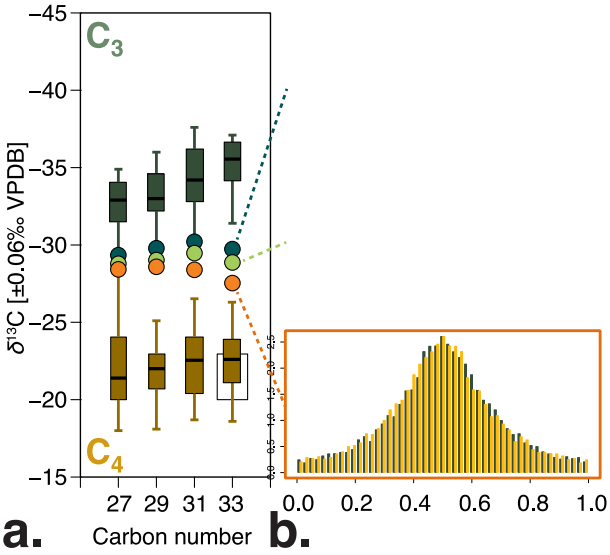

Figure 5: a) Carbon stable isotopic signatures ($\delta^{13}C$) of long chain *n*-alkanes C_{27}, C_{29}, C_{31} and C_{33} extracted from the P1 to P3 sediments: P1 (dark blue circles), P2 (light green circles) and P3 (orange circles) compared to boxplots showing the range of terrestrial leaf waxes values of C_3 (light and dark green) and C_4 (light and dark yellow) plants as described in the literature (wide light coloured boxes) and the arid zone subset (thin dark coloured boxes); **b)** change in end-members contribution over time, i.e., probability distributions of contribution from C_3 (dark green) and C_4 (yeallow) sources (SIAR).

(1-COLUMN FITTING IMAGE)

4. DISCUSSION

4.1 The organic molecular and stable isotopic fingerprint of drylands

These results show that it is possible to extract organic molecular fossil distributions and $\delta^{13}C$ of *n*-alkanes from lake sediments of low OM content in tropical arid ecosystems. The low total C content of the Fortescue Marsh sediments (<1 %) reflects the inherently low OM contents of modern Pilbara soils and is typical of dry stream-bed sediments (Bennett and Adams 1999; Ford et al. 2007; McIntyre et al. 2009b). The low concentration of the extracted bitumens (60–150 $\mu g \cdot g^{-1}$ of bulk P1–P3 sediment; Table 2) is also typical of OM-poor environments and oligotrophic aquatic systems (e.g., Kristen et al. 2010; Pautler et al. 2010; Fang et al. 2014). Sub-aerial exposition of the sediment during prolonged dry periods over recent millennia (Rouillard et al. 2016) would also have reduced OM preservation (Verschuren 1999). Nevertheless, saturated hydrocarbons typical of lipid metabolites were found in the upper 49 cm of the core (P1–P3; Fig. 2).

Our results also show that the molecular fossils can be used to characterise the major sources of sedimentary OM from the tropical arid system. The major aliphatic products identified in our sediments are indicative of predominantly terrestrial sources of OM at 14 Mile Pool (Fig. 2). The sediment of P1–3 consistently showed a homologous series of *n*-alkanes peaking at *n*-C_{31}. *n*-Alkanes are common hydrocarbon products of organic lake sediments derived from fatty acids, which are abundant components of epicuticular leaf waxes (Eglinton and Hamilton 1967) as well as many other biological systems and so are not always particularly source diagnostic of exact sources without additional evidence (e.g., stable isotopic composition). The relatively high abundances of *n*-alkanes in sediments across ecosystems are also due to a high structural recalcitrance to diagenesis (i.e., relatively high chemical stability, low solubility and are degraded slowly by microbes) compared to other functionalised biochemicals (Cranwell 1981; Schmidt et al. 2011). The unique lipid composition of many biological systems gives rise to *n*-alkanes of distinctive molecular distributions or stable isotope patterns that have thus been used previously to infer past hydroclimatic conditions across a range of environments (Castañeda and Schouten

493 2011; Garcin et al. 2012; Leng and Henderson 2013; Sun et al. 2013). For instance, chain length
494 distribution can be used to distinguish algal (short chain) from terrestrial, higher plant (long chain)
495 sources (Gelpi et al. 1970; Meyers and Ishiwatari 1993). A relatively high abundance of long chain
496 *n*-alkanes (>*n*-C_{25}) is often attributed to a high flux (or persistence) of terrestrially-derived OM
497 (Gelpi et al. 1970; Meyers and Ishiwatari 1993; Freeman and Colarusso 2001). While there are
498 non-terrestrial sources of long chain *n*-alkanes e.g., *Botryococcus braunii*, a phytoplanktonic alga
499 that is common in hypersaline or evaporitic lake settings (Grice et al. 1998), the long chain *n*-
500 alkanes prominent in each of the P1–P3 sediments also showed a distinctive odd/even carbon
501 number preference ($CPI_{23–33}$ = 3–6; Fig. 2) typical of terrestrial plant sources (allochthonous; e.g.,
502 Meyers 1997; Volkman et al. 1998; Freeman and Colarusso 2001; Rao et al. 2008).
503
504 The *n*-alkanes detected in the P1–P3 sediments (*n*-$C_{15\text{-}35}$ and CPI=2-12; Fig. 2 and Tables 2 & S1)
505 had a similar distribution to those reported in many other arid zone lake deposits (e.g., Garcin et
506 al. 2012). The $\delta^{13}C$ values were in the range −31 to −24 ‰ and displayed a 'saw-toothed' odd
507 versus even carbon numbered pattern (Fig. 4) that is very typical of a leaf wax source and linked
508 with higher plants biosynthesis (Collister et al. 1994; Zhou et al. 2010). The ephemeral reaches of
509 low-lying rivers are often important sinks for the terrestrial OM of upper catchment rivers,
510 streams and pools in arid environments (Jacobson et al. 2000; Fellman et al. 2013). Allochthonous
511 material transported from the catchment through floods or wind is one of the main drivers of
512 ecosystem metabolism in river networks (Sponseller et al. 2013). $\delta^{13}C$ of the 14 Mile Pool *n*-
513 alkanes (−32.3 to −26.6 ‰ Fig. 4) are consistent with observations from modern sediments (−35.9
514 to −26.8 ‰) from the arid, Sudano-Sahelian shrub savannah zone of Cameroon (Garcin et al.
515 2012). The CPI values of long-chain *n*-alkanes from dryland soils can vary with aridity (Krull et al.
516 2006; Rao et al. 2008; Luo et al. 2012) and can extend to higher values than those reported here
517 (e.g., 3–13, for *n*-C_{23}–*n*-C_{34} in several Chinese soils; Rao et al. 2008). Consequently, the molecular

518 evidence from the 14 Mile Pool sediments records a clear and dominant signature of the
519 terrestrial plant inputs from the surrounding arid catchment.
520
521 The shorter chain *n*-alkanes (*n*-$C_{17–26}$) of the sediments from 14 Mile Pool had lower $\delta^{13}C$ values
522 than the more abundant long-chain *n*-alkanes (*n*-$C_{27–35}$), implying that these *n*-alkanes derive from
523 a different source. The $\delta^{13}C$ of low MW *n*-alkanes (<*n*-C_{25}) in P1 and P3 were up to 1.5 ‰ lower
524 than co-occurring odd numbered high MW *n*-alkanes (>*n*-C_{27}; Fig. 4). These lower $\delta^{13}C$ values are
525 consistent with the lipids of algae or aquatic plants (Gelpi et al. 1970; Ficken et al. 2000), which
526 typically have lower $\delta^{13}C$ values than plant lipids (Chikaraishi and Naraoka 2003). Lower MW *n*-
527 alkanes typically derive from lower trophic organisms and aquatic producers such as
528 phytoplankton, benthic algae or aquatic macrophytes (e.g., Gelpi et al. 1970; Mead et al. 2005;
529 Aichner et al. 2010; Garcin et al. 2012). Macrophyte input was also indicated by P_{aq} values of 0.1–
530 0.3 for P1 and P3 sediments, though a mixture of the terrestrial and aquatic sources may also have
531 contributed to this value (Ficken et al. 2000). In the P2 sediments, the P_{aq} value was in the same
532 range (0.3) but the short chain *n*-alkanes were ~2 ‰ more positive than the long chain *n*-alkanes.
533 The $\delta^{13}C$ values of the P2 sediments were also similar to the $\delta^{13}C$ values of *n*-alkanes reported for
534 Lake Koucha sediments attributed to inputs from macrophytes and algae that had likely been
535 influenced by higher $\delta^{13}C$ of bicarbonates in the water body (e.g., Aichner et al. 2010; Kristen et al.
536 2010). Speculatively, the heavier short-chain *n*-alkanes in P2 may suggest a relatively stronger
537 groundwater influence during this period on the pool's hydrology and chemistry than present. This
538 observation would be consistent with the occurrence of one or several extreme floods inferred for
539 the periods (Rouillard et al. 2016), which would have enable an important rise in the water table
540 (Skrzypek et al. 2013) and favourable conditions for macrophytic growth, i.e. prolonged inundation
541 an a clear water column.
542

543 **4.2 *n*-alkanes as proxies of ecosystem carbon stocks**

544 By integrating the molecular abundance data with the Bayesian modelling of the stable isotopic
545 composition of the *n*-alkanes, we can assess that our results reflect the major vegetation types in
546 the catchment (C_3 and C_4) and hydrological processes at present and with hydroclimatic change
547 through the late Holocene in this subtropical arid zone. The particularly high abundance of *n*-C_{31} in
548 the sediments from 14 Mile Pool (Fig. 2) is consistent with the presently high catchment coverage
549 and biomass of warm-climate adapted C_4 grasses (~64 % of mainly *Triodia* spp.) relative to that of
550 woody C_3 plants, predominantly *Acacia* trees and shrubs (Fig. 1b; Adams et al. 2001). Though the
551 abundance of *n*-C_{31} alkane relative to *n*-C_{27} and *n*-C_{29} alkanes have been widely used to
552 differentiate grass-type (C_4) versus woody (C_3) plant contributions, recent research has shown that
553 caution is required with these estimates because the relative abundances of high molecular
554 weight *n*-alkanes can vary for both functional types (Bush and McInerney 2013). At 14 Mile Pool,
555 the occurrence of the very long-chain C_{33} (−26.6 ‰) and C_{35} (−24.0 ‰) *n*-alkanes and their
556 relatively high $\delta^{13}C$ signatures (Cf. Ave ~−28.5 ‰ of *n*-$C_{33–35}$); Fig. 4) are further evidence of C_4
557 plant input to the P1-3 sediments. Very long-chain *n*-alkanes are not only generally more
558 abundant in C_4 plants (e.g., Table 1), but their production may also be further enhanced under hot
559 and dry conditions (Rommerskirchen et al. 2006; Vogts et al. 2009). The $\delta^{13}C$ of *n*-alkanes in
560 Australian grassland soils usually reflects a C_4 prevalence (e.g., Krull et al. 2006).
561
562 The quantitative estimates from the stable isotope data suggests, however, the C_4 plants (41–50 %
563 median contribution in mixing model) might not have contributed as considerably to the 14 Mile
564 Pool sediments as might have been inferred from their current landscape dominance (64 %
565 aboveground biomass; Table 2; Fig. 5). This is because the riparian vegetation of the 14 Mile Pool
566 and broader riverine network (Fig. 1) may contribute substantial C_3 biomass resulting in a greater
567 contribution of ^{13}C-depleted *n*-alkanes than might be expected from the non-riparian C_3 plant

568 sources that predominantly inhabit arid environments. Disproportionally high riparian
569 contributions to organic sediment loads have previously been reported in other grasslands
570 dominated catchments: riparian trees in grasslands of sub-tropical Madagascar were thought
571 responsible for sedimentary OM with $\delta^{13}C$ values more than 6 ‰ lower than predicted from the
572 catchment vegetation composition (Marwick et al. 2014). Similarly, $\delta^{13}C$ trends in Holocene
573 sediments from a stream channel in southeastern Arizona were attributed to the establishment of
574 a riparian fringe and increasing contribution of C_3 herbaceous and woody vegetation over the
575 modern dominance of C_4 perennial grasses (Biedenbender et al. 2004). Preferential deposition of
576 riparian tree leaves to lake sediment and the importance of lateral OM contribution to streams
577 and rivers have also long been recognised in temperate environments (e.g., Conners and Naiman
578 1984; Seki et al. 2010). Viewed collectively, these findings suggest that the spatial structure of
579 catchment vegetation, rather than the cover or biomass only, strongly affects terrestrial OM
580 inputs to dryland sediments, and that the riparian contribution should particularly be taken into
581 consideration when interpreting vegetation changes in arid environments from sediment *n*-
582 alkanes $\delta^{13}C$.
583
584 If riparian plants (mainly C_3 and usually lower $\delta^{13}C$) are used as source material in the mixing
585 model, however, this would also likely change the $\delta^{13}C$ values of the C_3 end member, resulting in a
586 potential higher estimation of C_4 contribution to the Fortescue Marsh (Fig. 5). Response to plant
587 water stress, observed both globally (Weiguo et al. 2005; Diefendorf et al. 2010; Kohn 2010) and
588 along regional gradients (Schulze et al. 2014), can lead to an important $\delta^{13}C$ differential between
589 riparian and to non-riparian C_3 sources (Fig. 5). A summary of $\delta^{13}C$ foliar signatures from woody C_3
590 plants of this study's region showed that species from riparian fringes in the Pilbara have
591 significantly lower values (−4 ‰) than the foliage of homologue populations located on higher,
592 more water-stressed, parts of the landscape (Table S2; Fig. 6). Thus, C_3-sourced *n*-alkanes with

593 $\delta^{13}C$ values 4 ‰ lower than non-riparian sources would significantly decrease the model estimates
594 for the C_3 contribution and correspondingly project a higher C_4 input. A further complication to
595 consider is the substantial $\delta^{13}C$ offset that can occur between *n*-alkanes, leaf lipids and whole
596 leaves (Rieley et al. 1993; Bi et al. 2005; Diefendorf et al. 2011; Codron et al. 2013). The $\delta^{13}C$
597 dynamics related to water availability such as local growth conditions (Schouten et al. 1998;
598 Riebesell et al. 2000) and seasonal fluctuations (Lockheart et al. 1997) might also diverge for these
599 entities, and there might also be variation of behaviour within phenology (Diefendorf et al. 2011),
600 plant functional type (Shepherd and Wynne 2006; Bush and McInerney 2013; Cernusak et al.
601 2013), leaf ontogeny (Nguyen Tu et al. 2004) and phylogenetic group (Pedentchouk et al. 2008;
602 Diefendorf et al. 2011).
603

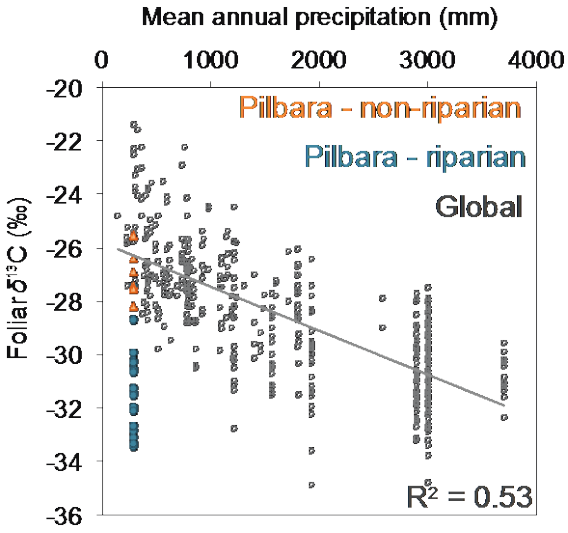

604
605
606 **Figure 6**: Relationship between foliar $\delta^{13}C$ and mean annual precipitation of woody (C_3) riparian
607 (filled blue circles) and non-riparian (filled orange triangles) vegetation from the Pilbara (collected
608 between 1997 and 2013 by the Ecosystem Research Group at The University of Western Australia;
609 see Table S2 for more information of species and sampling of the Pilbara dataset) compared to the
610 global distribution (open grey circles; modified from Diefendorf et al. 2010).
611 (1-COLUMN FITTING IMAGE)

In low water flow systems of arid zones, additional consideration of the complex deposition processes across timescales may be important from the reconstruction of past catchment vegetation from sediment records. For instance, leaf litter may accumulate in isolated pools or onto dry stream beds (McIntyre et al. 2009b) until transportation in various stages of decay downstream by heavy and unpredictable summer floods (e.g., Robertson et al. 2001; Francis and Sheldon 2002; Mladenov et al. 2007). Ecological 'booms' following large rains contrast prolonged periods of low productivity in arid catchments (Collins et al. 2008; McGrath et al. 2012; Kanniah et al. 2013). High energy floods in arid regions can lead to a wide dispersal of higher plants across the landscape and the increased likelihood following mortality of rapid photodegradation (i.e., minimal tree canopy or litter shelter from sustained UV radiation) or consumption by the termites prolific in Australian savannahs (e.g., Holt et al. 1987; Chen et al. 2003; Austin et al. 2004). The development of complementary indicators and of additional sediment records with finer temporal resolutions from the arid zone sediment may help towards a better understanding of these complex spatio-temporal patterns of OM deposition. Clearly, the range of $\delta^{13}C$ values for *n*-alkanes from different sources needs to be better defined in space and time for more precise quantitative mixing model estimates of contributions of different lipid sources to lake environments and reconstruction of vegetation cover in catchments.

The molecular data also showed a small but distinctive aquatic contribution in P1 that was not detected in older sediments (Fig. 2), particularly as determined from the lower chain length *n*-alkanes (Gelpi et al. 1970; Mead et al. 2005; Aichner et al. 2010; Garcin et al. 2012). The significantly lower $\delta^{13}C$ value of *n*-C_{17} compared to the larger *n*-alkanes (Fig. 4) further suggests a cyanobacterial contribution to sediment OM (Kristen et al. 2010). Cyanobacterial mats are common in freshwater/brackish limnological conditions and high pH environments (Rontani and

637 Volkman 2005) and microbial mats were visually evident at the sediment/water interface of the
638 pool during several field surveys.
639
640 Steroids, generally originating from eukaryotic organisms such as higher plants or algae, as well as
641 hopanoids, which are typically associated with microbial inputs (Aichner et al. 2010), were
642 detected in all sediments. Their relative abundances were generally low (Fig. 3), though higher in
643 P2 and P3 (steroids 7–8 % TIC signal; hopanoids 4–6 %) than P1 (steroids 1.3 %; hopanoids 2.6 %),
644 perhaps on account of greater diagenetic reduction of the poly-hydroxy functionalities of their
645 biochemical form (Peters et al. 2005). Sediments of P1 showed a more diverse assemblage of
646 these products (Fig. 2 and 3), including unusual series of low molecular weight steranes ($C_{19–22}$)
647 and tri- and tetracyclic terpanes (C_{19}–C_{24}). The greater biomarker diversity evident in P1 suggests
648 the recent wetter conditions (Rouillard et al. 2016) favoured a more complex microbial pool that
649 may also have supported greater heterotroph reworking of the OM (i.e., resulting in overall lower
650 abundance). A similar series of low molecular weight steranes (extending to slightly large Cn) were
651 reported in relatively high concentrations in immature evaporitic marl sediments of the Jinxian
652 Sag, Bohai Bay Basin, North China (Lu et al. 2009) and generally attributed to early diagenetic
653 products of microbial sources in a carbonate environment (Erik 2011; Oliveira et al. 2012). The
654 higher steroid to hopanoid ratio detected in P2 and P3 (Fig. 3) is also consistent with a greater
655 representation of terrestrially-derived OM during those periods compared to the more recent P1
656 sediments (Tissot and Welte 1984).
657
658 **4.3 Do sediment *n*-alkanes reflect hydroclimatic change at the Fortescue Marsh in the late**
659 **Holocene?**
660 The final objective of this study was to assess whether the distribution of biomarkers and $\delta^{13}C$
661 values of *n*-alkanes from the sediment reflected ecosystem responses to regional hydroclimatic

change over the late Holocene (last ~2000 years). While we previously discussed our molecular record against the hydroclimatic reconstruction at the Fortescue Marsh (Rouillard et al., 2016), here we also compare our findings to other regional palaeoecological records focussing on OM and vegetation changes for the four periods investigated (P1-P4). The very low organic content of the older section (P4) core—below the detection limit of presently applied GC-MS analyses—is consistent with notably drier conditions in the inland Pilbara region more than 1300 years ago compared to present (Rouillard et al. 2016). Marine sediment pollen records (van der Kaars et al. 2006) and coastal speleothem records (Denniston et al. 2013) have revealed a decrease in C_3 vegetation across northwest Australia since the mid-Holocene, which has been attributed to a drier climate, equivalent to a decrease of ~150 mm·year^{-1} in mean coastal rainfall. Terrestrial pollen records further east also suggest a decline in effective precipitation (EP) in tropical northern Australia (Gulf of Carpenteria) from 4000–3500 years BP followed by an increase in EP over the last 2000 years (Schulmeister and Lees 1995). Recent evaluation of a sediment record from the eastern Kimberley has also indicated increasing woody vegetation following rapid increased fluvial sedimentation around CE 650–850 (McGowan et al. 2012).

Given the differences evident in the molecular and stable isotopic distributions of lipid derived *n*-alkanes in sediments from the oldest (P3) to the youngest (P1), we might conclude that vegetation structure and composition in the catchment have been broadly consistent in the region for the last ~1300 years (Table 2; Fig. 2). Nonetheless, other hydroclimatic reconstructions based on physical and other biogeochemical characteristics indicate conditions in the region have become progressively wetter since ~ CE 700 (Rouillard et al. 2016 and references therein), including the more coarsely resolved studies mentioned earlier. In particular, the near-permanently inundated conditions under a wetter recent climate in the last ~20 years inferred from multiple sediment indicators at the site (P1; Rouillard et al. 2016) are corroborated by reconstructions from tree-ring

687 and stable isotopes chronologies in the catchment (Cullen and Grierson 2007; O'Donnell et al.
688 2015), and by instrumental data and modelling from satellite imagery and rainfall timeseries
689 (Rouillard et al. 2015; Shi et al. 2008). Under wetter (or less arid) conditions we might expect i) an
690 expanded riparian fringe; ii) a greater catchment representation of C_3 plants; and/or iii) alleviated
691 water stress of this vegetation. Such a scenario would account for the significantly lower $\delta^{13}C$
692 values evident in the shallower sediment (P1 < P2 < P3; total variance of ~2 ‰; Fig. 5). Similar 2–
693 3 ‰ magnitude shifts in the $\delta^{13}C$ values of long ($C_{29–33}$) odd chain *n*-alkanes from Lake Malawi,
694 equatorial East Africa, was reported to reflect a 15 % increase in C_4 vegetation and millennial
695 drought during the Younger Dryas cold period (Castañeda et al. 2007), and in the $\delta^{13}C$ of long
696 chain *n*-alkanoic acids extracted from marine sediment was associated to a ~20 % variability in the
697 C_3 and C_4 vegetation of northeast Africa (Feakins et al. 2007). The higher relative abundances of
698 lower MW *n*-alkanes are also indicative of aquatic sources (Fig. 3). Consequently, sediment
699 biomarkers and *n*-alkanes $\delta^{13}C$ from the 14 Mile Pool effectively reflected the local response of
700 vegetation to hydrological and regional hydroclimatic change in the late Holocene, even though
701 this change may have been relatively modest on a catchment scale. Take together, our results
702 show that improved baselines and a careful consideration of the complex spatial and temporal
703 interaction between plants and water in arid tropical ecosystems are crucial for an appropriate
704 interpretation of past vegetation dynamics from molecular proxies.
705
706 **5. CONCLUSIONS**
707 The major organic input to sediments from an episodic wetland (Fortescue Marsh, Pilbara) (i.e.,
708 aquatic microflora, C_4 grasses, and C_3 plants originating at least partly from a significant riparian
709 fringe) could be revealed from the trace levels of aliphatic hydrocarbon compounds (including *n*-
710 alkanes, branched alkanes, hopanoids and steroids) detected in them. A temporal flux of some
711 sources was also evident. The stable isotopic signatures measured for several of the more

712 abundant *n*-alkanes provided additional C source information that can be useful for paleoclimate
713 reconstructions. Particularly, the relatively lower $\delta^{13}C$ values of long chain *n*-alkanes in modern
714 sediments reflected the emergence of wetter conditions through the late Holocene, and
715 particularly over recent decades. Though we highlight limitations and caution in interpreting
716 organic geochemical signals in sediments from tropical drylands, this approach provides valuable
717 information for the interpretation of arid paleoenvironmental records globally. Of note, these data
718 can serve as relatively modern analogues for the characteristics of biomarker records that have
719 been deposited during ancient dry phases recorded in very long (>100,000 yrs)
720 paleoenvironmental records, such as the ongoing projects of the International Continental
721 Scientific Drilling Program (http://www.icdp-online.org/home/): the Hominin Sites and Paleolakes
722 Drilling Project (HSPDP) in East Africa, the Lake Chad Deep Drilling (CHADRILL) in North Africa, the
723 Lake Petén Itza in Guatemala and the Lake Chalco in Mexico. Regionally, more extensive and
724 representative organic geochemical datasets, particularly of *n*-alkane $\delta^{13}C$ signatures from a range
725 of sources (e.g. riparian vegetation) common across northern and inland Australia and other sub-
726 tropical drylands, will help improve the accuracy and uncertainty of mixing models to reconstruct
727 past vegetation contributions quantitatively in these relatively underrepresented regions.
728
729

730 **ACKNOWLEDGEMENTS**

731 We thank D. Thomas (Oxford Uni.), D. Vershuren (Ghent Uni.) and J. Tibby (Uni. Adelaide) for their
732 comments, which contributed to improve the manuscript. This research was supported by the
733 Australian Research Council (ARC) in partnership with Rio Tinto (LP120100310). A. Rouillard was
734 supported by the Australian Government and UWA via an International Postgraduate Research
735 Scholarships (IPRS), Australian Postgraduate Award (APA) and a UWA Safety Top-up Scholarship,
736 as well as by the Canadian and Québec governments via a Natural Sciences and Engineering
737 Research Council (NSERC) and Fonds québécois de la recherche sur la nature et les technologies
738 (FQRNT) graduate scholarships. G. Skrzypek participation was supported by an ARC Future
739 Fellowship (FT110100352). K. Grice participation was supported by an ARC DORA fellowship
740 (DP130100577) and ARC LIEFP grant for CSIA. Data for Fig. 6 (Table S2) were cumulatively
741 collected by Ecosystem Research Group members R. Argus, L. Cullen, J. Graham, P. Landman, R.
742 McIntyre, E. McLean and G. Page. Laboratory support at Curtin University was kindly provided by
743 Robert Lockhart and the WA-OIGC team. Glenn Kirkpatrick and Douglas Ford provided invaluable
744 support in the field (UWA). We also thank Adrienne Marquis (DPaw) for her contribution of plant
745 survey information from the Fortescue Marsh. We ultimately acknowledge the kind field support
746 of Murray and Ray Kennedy (Roy Hill Station), Sue and Lee Bickell (Marillana Station), Barry and
747 Bella Grett (Ethel Creek Station) and Victor and Larissa Gleeson (Mulga Downs Station).

748

749

750 **REFERENCES**

751 Adams M, Grierson P, Bussau A, Dorling K (2001) Biomass and carbon in vegetation of the Pilbara
752 region, Western Australia. Dissertation, The University of Western Australia

753 Aichner B, Wilkes H, Herzschuh U, Mischke S, Zhang C (2010) Biomarker and compound-specific
754 $\delta^{13}C$ evidence for changing environmental conditions and carbon limitation at Lake Koucha,
755 eastern Tibetan Plateau. Journal of Paleolimnology 43:873–899

756 Argus RE, Colmer TD, Grierson PF (2015) Early physiological flood tolerance is followed by slow
757 post-flooding root recovery in the dryland riparian tree *Eucalyptus camaldulensis* subsp.
758 *refulgens*. Plant, Cell & Environment 38:1189–1199

759 Argus R, Page G, Grierson P (2014) Impacts of artificial inundation of ephemeral creek beds on
760 mature riparian eucalypts in semi-arid northwest Australia. EGU General Assembly
761 Conference Abstracts 16:10098

762 Atahan P, Heijnis H, Dodson J, Grice K, Le M, Pierre, Taffs K, Hembrow S, Woltering M, Zawadzki A
763 (2015) Pollen, biomarker and stable isotope evidence of late Quaternary environmental
764 change at Lake McKenzie, southeast Queensland. Journal of Paleolimnology 53:139–156

765 Austin AT, Yahdjian L, Stark JM, Belnap J, Porporato A, Norton U, Ravetta DA, Schaeffer SM (2004)
766 Water pulses and biogeochemical cycles in arid and semiarid ecosystems. Oecologia
767 141:221–235

768 Barr C, Tibby J, Gell P, Tyler J, Zawadzki A, Jacobsen GE (2014) Climate variability in south-eastern
769 Australia over the last 1500 years inferred from the high-resolution diatom records of two
770 crater lakes. Quaternary Science Reviews 95:115–131

771 Battin TJ, Kaplan LA, Findlay S, Hopkinson CS, Marti E, Packman AI, Newbold JD, Sabater F (2008)
772 Biophysical controls on organic carbon fluxes in fluvial networks. Nature Geoscience 1:95–
773 100

774 Beard JS (1975) The vegetation of the Pilbara area. Vegetation Survey of Western Australia 1:1 000
775 000 Vegetation Series, Map and explanatory notes

776 Bennett LT, Adams MA (2001) Response of a perennial grassland to nitrogen and phosphorus
777 additions in sub-tropical, semi-arid Australia. Journal of Arid Environments 48:289–308

778 Bessems I, Verschuren D, Russell JM, Hus J, Mees F, Cumming BF (2008) Palaeolimnological
779 evidence for widespread late 18th century drought across equatorial East Africa.
780 Palaeogeography, Palaeoclimatology, Palaeoecology 259:107–120

781 Bi X, Sheng G, Liu X, Li C, Fu J (2005) Molecular and carbon and hydrogen isotopic composition of
782 *n*-alkanes in plant leaf waxes. Organic Geochemistry 36:1405–1417

783 Biedenbender SH, McClaran MP, Quade J, Weltz MA (2004) Landscape patterns of vegetation
784 change indicated by soil carbon isotope composition. Geoderma 119:69–83

785 Birks HJB, Birks HH (2016) How have studies of ancient DNA from sediments contributed to the
786 reconstruction of Quaternary floras? New Phytologist 209:499–506

787 Blumer M (1957) Removal of elemental sulfur from hydrocarbon fractions. Analytical Chemistry
788 29:1039–1041

789 Bray EE, Evans ED (1961) Distribution of *n*-paraffins as a clue to recognition of source beds.
790 Geochimica et Cosmochimica Acta 22:2–15

791 Brodie CR, Casford JSL, Lloyd JM, Leng MJ, Heaton THE, Kendrick CP, Yongqiang Z (2011) Evidence
792 for bias in C/N, δ^{13}C and δ^{15}N values of bulk organic matter, and on environmental

793 interpretation, from a lake sedimentary sequence by pre-analysis acid treatment methods.
794 Quaternary Science Reviews 30:3076–3087

795 Bush RT, McInerney FA (2013) Leaf wax *n*-alkane distributions in and across modern plants:
796 Implications for paleoecology and chemotaxonomy. Geochimica et Cosmochimica Acta
797 117:161–179

798 Carolin RC, Jacobs SWL, Vesk M (1982) The chlorenchyma of some members of the Salicornieae
799 (Chenopodiaceae). Australian Journal of Botany 30:387–392

800 Castañeda IS, Werne JP, Johnson TC, Filley TR (2009a) Late Quaternary vegetation history of
801 southeast Africa: The molecular isotopic record from Lake Malawi. Palaeogeography,
802 Palaeoclimatology, Palaeoecology 275:100–112

803 Castañeda IS, Mulitza S, Schefuß E, dos Santos RAL, Damsté JSS, Schouten S (2009b) Wet phases in
804 the Sahara/Sahel region and human migration patterns in North Africa. Proceedings of the
805 National Academy of Sciences 106:20159–20163

806 Castañeda IS, Schouten S (2011) A review of molecular organic proxies for examining modern and
807 ancient lacustrine environments. Quaternary Science Reviews 30:2851–2891

808 Castañeda IS, Werne JP, Johnson TC (2007) Wet and arid phases in the southeast African tropics
809 since the Last Glacial Maximum. Geology 35:823–826

810 Cernusak LA, Ubierna N, Winter K, Holtum JAM, Marshall JD, Farquhar GD (2013) Environmental
811 and physiological determinants of carbon isotope discrimination in terrestrial plants. New
812 Phytologist 200:950–965

813 Chen X, Hutley LB, Eamus D (2003) Carbon balance of a tropical savanna of northern Australia.
814 Oecologia 137:405–416

Chikaraishi Y, Naraoka H (2003) Compound-specific δD-δ^{13}C analyses of *n*-alkanes extracted from terrestrial and aquatic plants. Phytochemistry 63:361–371

Codron J, Lee-Thorp JA, Sponheimer M, Codron D (2013) Plant stable isotope composition across habitat gradients in a semi-arid savanna: implications for environmental reconstruction. Journal of Quaternary Science 28:301–310

Collins SL, Sinsabaugh RL, Crenshaw C, Green L, Porras-Alfaro A, Stursova M, Zeglin LH (2008) Pulse dynamics and microbial processes in aridland ecosystems. Journal of Ecology 96:413–420

Collister JW, Rieley G, Stern B, Eglinton G, Fry B (1994) Compound-specific δ^{13}C analyses of leaf lipids from plants with differing carbon dioxide metabolisms. Organic Geochemistry 21:619–627

Conners ME, Naiman RJ (1984) Particulate allochthonous inputs: relationships with stream size in an undisturbed watershed. Canadian Journal of Fisheries and Aquatic Sciences 41:1473–1484

Cranwell PA (1981) Diagenesis of free and bound lipids in terrestrial detritus deposited in a lacustrine sediment. Organic Geochemistry 3:79–89

Cullen LE, Adams MA, Anderson MJ, Grierson PF (2008) Analyses of δ^{13}C and δ^{18}O in tree rings of *Callitris columellaris* provide evidence of a change in stomatal control of photosynthesis in response to regional changes in climate. Tree Physiology 28:1525–1533

Cullen LE, Grierson PF (2007) A stable oxygen, but not carbon, isotope chronology of Callitris columellaris reflects recent climate change in north-western Australia. Climatic Change 85:213–229

Cushing EJ (1967) Evidence for differential pollen preservation in late Quaternary sediments in Minnesota. Review of Palaeobotany and Palynology 4:87–101

837 Denniston RF, Asmerom Y, Lachniet M, Polyak VJ, Hope P, An N, Rodzinyak K, Humphreys WF
838 (2013) A Last Glacial Maximum through middle Holocene stalagmite record of coastal
839 Western Australia climate. Quaternary Science Reviews 77:101–112

840 Diefendorf AF, Freeman KH, Wing SL, Graham HV (2011) Production of *n*-alkyl lipids in living plants
841 and implications for the geologic past. Geochimica et Cosmochimica Acta 75:7472–7485

842 Diefendorf AF, Mueller KE, Wing SL, Koch PL, Freeman KH (2010) Global patterns in leaf ^{13}C
843 discrimination and implications for studies of past and future climate. Proceedings of the
844 National Academy of Sciences 107:5738–5743

845 Duan Y, Wu Y, Cao X, Zhao Y, Ma L (2014) Hydrogen isotope ratios of individual *n*-alkanes in plants
846 from Gannan Gahai Lake (China) and surrounding area. Organic Geochemistry 77:96–105

847 Dubois N, Oppo DW, Galy VV, Mohtadi M, van dK, Sander, Tierney JE, Rosenthal Y, Eglinton TI,
848 Lückge A, Linsley BK (2014) Indonesian vegetation response to changes in rainfall seasonality
849 over the past 25,000 years. Nature Geoscience 4:513–517

850 Eglinton G, Hamilton RJ (1967) Leaf epicuticular waxes. Science 156:1322–1335

851 Erik YN (2011) Hydrocarbon generation potential and Miocene—Pliocene paleoenvironments of
852 the Kangal Basin (Central Anatolia, Turkey). Journal of Asian Earth Sciences 42:1146–1162

853 Fang J, Wu F, Xiong Y, Li F, Du X, An D, Wang L (2014) Source characterization of sedimentary
854 organic matter using molecular and stable carbon isotopic composition of *n*-alkanes and
855 fatty acids in sediment core from Lake Dianchi, China. Science of The Total Environment
856 473:410–421

857 Feakins SJ, Eglinton TI, demenocal PB (2007) A comparison of biomarker records of northeast
858 African vegetation from lacustrine and marine sediments (ca. 3.40 Ma). Organic
859 Geochemistry 38:1607–1624

860 Fellman JB, Petrone KC, Grierson PF (2013) Leaf litter age, chemical quality, and photodegradation
861 control the fate of leachate dissolved organic matter in a dryland river. Journal of Arid
862 Environments 89:30–37

863 Ficken KJ, Li B, Swain DL, Eglinton G (2000) An *n*-alkane proxy for the sedimentary input of
864 submerged/floating freshwater aquatic macrophytes. Organic Geochemistry 31:745–749

865 Finlay JC, Kendall C (2008) Stable isotope tracing of temporal and spatial variability in organic
866 matter sources to freshwater ecosystems. In: Michener R, Lajtha K (eds) Stable isotopes in
867 ecology and environmental science. Wiley-Blackwell, Hoboken, Oxford, UK, pp 283-333

868 Ford DJ, Cookson WR, Adams MA, Grierson PF (2007) Role of soil drying in nitrogen mineralization
869 and microbial community function in semi-arid grasslands of north-west Australia. Soil
870 Biology and Biochemistry 39:1557–1569

871 Francis C, Sheldon F (2002) River Red Gum (*Eucalyptus camaldulensis* Dehnh.) organic matter as a
872 carbon source in the lower Darling River, Australia. Hydrobiologia 481:113–124

873 Freeman KH, Colarusso LA (2001) Molecular and isotopic records of C4 grassland expansion in the
874 late Miocene. Geochimica et Cosmochimica Acta 65:1439–1454

875 Garcin Y, Schwab VF, Gleixner G, Kahmen A, Todou G, Séné O, Onana JM, Achoundong G, Sachse D
876 (2012) Hydrogen isotope ratios of lacustrine sedimentary *n*-alkanes as proxies of tropical
877 African hydrology: Insights from a calibration transect across Cameroon. Geochimica et
878 Cosmochimica Acta 79:106–126

879 Gelpi E, Schneider H, Mann J, Oro J (1970) Hydrocarbons of geochemical significance in
880 microscopic algae. Phytochemistry 9:603–612

881 Gergis J, Hope P, Abram N, Henley B (2014) Australasia's climate variability: clues drawn from
882 paleoclimate and model data over the last 2000 years. PAGES Magazine 22:101

Grice K, Schouten S, Nissenbaum A, Charrach J, Sinninghe D, Jaap S (1998) A remarkable paradox: sulfurised freshwater algal (*Botryococcus braunii*) lipids in an ancient hypersaline euxinic ecosystem. Organic Geochemistry 28:195–216

Hoffmann B, Kahmen A, Cernusak LA, Arndt SK, Sachse D (2013) Abundance and distribution of leaf wax *n*-alkanes in leaves of *Acacia* and *Eucalyptus* trees along a strong humidity gradient in northern Australia. Organic Geochemistry 62:62–67

Holt JA (1987) Carbon mineralization in semi-arid northeastern Australia: the role of termites. Journal of Tropical Ecology 3:255–263

Hopkins JB, Ferguson JM (2012) Estimating the diets of animals using stable isotopes and a comprehensive Bayesian mixing model. PLoS One 7:e28478

Huxman TE, Snyder KA, Tissue D, Leffler AJ, Ogle K, Pockman WT, Sandquist DR, Potts DL, Schwinning S (2004) Precipitation pulses and carbon fluxes in semiarid and arid ecosystems. Oecologia 141:254–268

Jacobson PJ, Jacobson KM, Angermeier PL, Cherry DS (2000) Variation in material transport and water chemistry along a large ephemeral river in the Namib Desert. Freshwater Biology 44:481–491

Kanniah KD, Beringer J, Hutley LB (2013) Response of savanna gross primary productivity to interannual variability in rainfall: Results of a remote sensing based light use efficiency model. Progress in Physical Geography 37:642–663

Kennard MJ, Pusey BJ, Olden JD, Mackay SJ, Stein JL, Marsh N (2010) Classification of natural flow regimes in Australia to support environmental flow management. Freshwater Biology 55:171–193

905 Kohn MJ (2010) Carbon isotope compositions of terrestrial C3 plants as indicators of (paleo)
906 ecology and (paleo) climate. Proceedings of the National Academy of Sciences 107:19691–
907 19695

908 Kristen I, Wilkes H, Vieth A, Zink K-G, Plessen B, Thorpe J, Partridge TC, Oberhänsli H (2010)
909 Biomarker and stable carbon isotope analyses of sedimentary organic matter from Lake
910 Tswaing: evidence for deglacial wetness and early Holocene drought from South Africa.
911 Journal of Paleolimnology 44:143–160

912 Krull E, Sachse D, Mügler I, Thiele A, Gleixner G (2006) Compound-specific $\delta^{13}C$ and $\delta^{2}H$ analyses of
913 plant and soil organic matter: A preliminary assessment of the effects of vegetation change
914 on ecosystem hydrology. Soil Biology and Biochemistry 38:3211–3221

915 Krull ES, Skjemstad JO, Burrows WH, Bray SG, Wynn JG, Bol R, and S, Leonie, Harms B (2005)
916 Recent vegetation changes in central Queensland, Australia: Evidence from $\delta^{13}C$ and ^{14}C
917 analyses of soil organic matter. Geoderma 126:241–259

918 Kuhn TK, Krull ES, Bowater A, Grice K, Gleixner G (2010) The occurrence of short chain *n*-alkanes
919 with an even over odd predominance in higher plants and soils. Organic Geochemistry
920 41:88–95

921 Leng MJ, Henderson ACG (2013) Recent advances in isotopes as palaeolimnological proxies.
922 Journal of Paleolimnology 49:481–496

923 Lockheart MJ, Van B, Pim F, Evershed RP (1997) Variations in the stable carbon isotope
924 compositions of individual lipids from the leaves of modern angiosperms: implications for
925 the study of higher land plant-derived sedimentary organic matter. Organic Geochemistry
926 26:137–153

927 Lowe JJ (1982) Three Flandrian Pollen Profiles from the Teith Valley, Perthshire, Scotland. II.
928 Analysis of Deteriorated Pollen. New Phytologist 90:371–385

929 Lu H, Chen T, Grice K, Greenwood P, Peng P, Sheng G (2009) Distribution and significance of novel
930 low molecular weight sterenes in an immature evaporitic sediment from the Jinxian Sag,
931 North China. Organic Geochemistry 40:902–911

932 Luo P, Peng P, Lü H, Zheng Z, Wang X (2012) Latitudinal variations of CPI values of long-chain *n*-
933 alkanes in surface soils: Evidence for CPI as a proxy of aridity. Science China Earth Sciences
934 55:1134–1146

935 Marwick TR, Borges AV, Van A, Kristof, Darchambeau F, Bouillon S (2014) Disproportionate
936 Contribution of Riparian Inputs to Organic Carbon Pools in Freshwater Systems. Ecosystems
937 17:974–989

938 McGowan H, Marx S, Moss P, Hammond A (2012) Evidence of ENSO mega-drought triggered
939 collapse of prehistory Aboriginal society in northwest Australia. Geophysical Research Letters
940 39:L22702, 1–5

941 McGrath GS, Sadler R, Fleming K, Tregoning P, Hinz C, Veneklaas EJ (2012) Tropical cyclones and
942 the ecohydrology of Australia's recent continental-scale drought. Geophysical Research
943 Letters 39:L03404, 1–16

944 McIntyre RES, Adams MA, Ford DJ, Grierson PF (2009a) Rewetting and litter addition influence
945 mineralisation and microbial communities in soils from a semi-arid intermittent stream. Soil
946 Biology and Biochemistry 41:92–101

947 McIntyre RES, Adams MA, Grierson PF (2009b) Nitrogen mineralization potential in rewetted soils
948 from a semi-arid stream landscape, north-west Australia. Journal of Arid Environments
949 73:48–54

McKenzie NL, van Leeuwen S, Pinder AM (2009) Introduction to the Pilbara biodiversity survey, 2002-2007. Records of the Western Australian Museum, Supplement 78:3–89

McKirdy DM, Thorpe CS, Haynes DE, Grice K, Krull ES, Halverson GP, Webster LJ (2010) The biogeochemical evolution of the Coorong during the mid-to late Holocene: An elemental, isotopic and biomarker perspective. Organic Geochemistry 41:96–110

Mead R, Xu Y, Chong J, Jaffé R (2005) Sediment and soil organic matter source assessment as revealed by the molecular distribution and carbon isotopic composition of *n*-alkanes. Organic Geochemistry 36:363–370

Meyers PA (1997) Organic geochemical proxies of paleoceanographic, paleolimnologic, and paleoclimatic processes. Organic Geochemistry 27:213–250

Meyers PA, Ishiwatari R (1993) Lacustrine organic geochemistry-an overview of indicators of organic matter sources and diagenesis in lake sediments. Organic Geochemistry 20:867–900

Mladenov N, McKnight DM, Wolski P, Murray-Hudson M (2007) Simulation of DOM fluxes in a seasonal floodplain of the Okavango Delta, Botswana. Ecological Modelling 205:181–195

Moir-Barnetson L (2014) Ecophysiological responses to changes in salinity and water availability in stem-succulent halophytes (*Tecticornia* spp.) from an ephemeral salt lake. Plant Biology, Ph.D., The University of Western Australia, 208 pp.

Nguyen Tu TT, Derenne S, Largeau C, Bardoux G, Mariotti A (2004) Diagenesis effects on specific carbon isotope composition of plant *n*-alkanes. Organic Geochemistry 35:317–329

O'Donnell AJ, Boer MM, McCaw WL, Grierson PF (2011) Climatic anomalies drive wildfire occurrence and extent in semi-arid shrublands and woodlands of southwest Australia. Ecosphere 2:Art127, 1–15

O'Donnell AJ, Cook ER, Palmer JG, Turney CSM, Page GFM, Grierson PF (2015) Tree Rings Show Recent High Summer-Autumn Precipitation in Northwest Australia Is Unprecedented within the Last Two Centuries. PloS one 10:e0128533

Oliveira CR, Ferreira AA, Oliveira CJF, Azevedo DA, Santos N, Eugênio V, Aquino N, Francisco R (2012) Biomarkers in crude oil revealed by comprehensive two-dimensional gas chromatography time-of-flight mass spectrometry: depositional paleoenvironment proxies. Organic Geochemistry 46:154–164

Pagès A, Grice K, Ertefai T, Skrzypek G, Jahnert R, Greenwood P (2014) Organic geochemical studies of modern microbial mats from Shark Bay: Part I: Influence of depth and salinity on lipid biomarkers and their isotopic signatures. Geobiology 12:469–487

Pagès A, Grice K, Welsh DT, Teasdale PT, Van K, Martin J, Greenwood P (2015) Lipid Biomarker and Isotopic Study of Community Distribution and Biomarker Preservation in a Laminated Microbial Mat from Shark Bay, Western Australia. Microbial Ecology 70:459–472

Parnell AC, Inger R, Bearhop S, Jackson AL (2010) Source partitioning using stable isotopes: coping with too much variation. PLOS one 5:e9672

Pautler BG, Austin J, Otto A, Stewart K, Lamoureux SF, Simpson MJ (2010) Biomarker assessment of organic matter sources and degradation in Canadian High Arctic littoral sediments. Biogeochemistry 100:75–87

Pedentchouk N, Sumner W, Tipple B, Pagani M (2008) δ^{13}C and δD compositions of *n*-alkanes from modern angiosperms and conifers: An experimental set up in central Washington State, USA. Organic Geochemistry 39:1066–1071

993 Peters KE, Walters CC, Moldowan JM (2005) (eds) The biomarker guide: Volume 1, Biomarkers and
994 isotopes in the environment and human history. Cambridge University Press, Cambridge, 471
995 pp

996 Phillips DL, Koch PL (2002) Incorporating concentration dependence in stable isotope mixing
997 models. Oecologia 130:114–125

998 Puttock A, Dungait JAJ, Bol R, and D, Elizabeth R, Macleod CJA, Brazier RE (2012) Stable carbon
999 isotope analysis of fluvial sediment fluxes over two contrasting C4-C3 semi-arid vegetation
1000 transitions. Rapid Communications in Mass Spectrometry 26:2386–2392

1001 Qin C, Yang B, Bräuning A, Grießinger J, Wernicke J (2015) Drought signals in tree-ring stable
1002 oxygen isotope series of Qilian juniper from the arid northeastern Tibetan Plateau. Global
1003 and Planetary Change 125:48–59

1004 Rao Z, Jia G, Zhu Z, Wu Y, Zhang J (2008) Comparison of the carbon isotope composition of total
1005 organic carbon and long-chain *n*-alkanes from surface soils in eastern China and their
1006 significance. Chinese Science Bulletin 53:3921–3927

1007 Reid MA, Ogden R, Thoms MC (2011) The influence of flood frequency, geomorphic setting and
1008 grazing on plant communities and plant biomass on a large dryland floodplain. Journal of
1009 Arid Environments 75:815–826

1010 Riebesell U, Revill AT, Holdsworth DG, Volkman JK (2000) The effects of varying CO2 concentration
1011 on lipid composition and carbon isotope fractionation in *Emiliania huxleyi*. Geochimica et
1012 Cosmochimica Acta 64:4179–4192

1013 Rieley G, Collister JW, Stern B, Eglinton G (1993) Gas chromatography/isotope ratio mass
1014 spectrometry of leaf wax *n*-alkalines from plants of differing carbon dioxide metabolisms.
1015 Rapid Communications in Mass Spectrometry 7:488–491

1016 Robertson AI, Bacon P, Heagney G (2001) The responses of floodplain primary production to flood
1017 frequency and timing. Journal of Applied Ecology 38:126–136

1018 Romero-Viana L, Kienel U, Sachse D (2012) Lipid biomarker signatures in a hypersaline lake on
1019 Isabel Island (Eastern Pacific) as a proxy for past rainfall anomaly (1942-2006AD).
1020 Palaeogeography, Palaeoclimatology, Palaeoecology 350-352:49–61

1021 Rommerskirchen F, Plader A, Eglinton G, Chikaraishi Y, Rullkötter J (2006) Chemotaxonomic
1022 significance of distribution and stable carbon isotopic composition of long-chain alkanes and
1023 alkan-1-ols in C4 grass waxes. Organic Geochemistry 37:1303–1332

1024 Rontani J-F, Volkman JK (2005) Lipid characterization of coastal hypersaline cyanobacterial mats
1025 from the Camargue (France). Organic Geochemistry 36:251–272

1026 Rouillard A, Skrzypek G, Dogramaci S, Turney C, Grierson PF (2015) Impacts of high inter-annual
1027 variability of rainfall on a century of extreme hydrologic regime of northwest Australia.
1028 Hydrology and Earth System Sciences 19:2057–2078

1029 Rouillard, A, Skrzypek, G, Turney, C, Dogramaci, S, Hua, Q, Zawadzki, A, Reeves, J, O'Donnell, A,
1030 and Grierson, P (2016). Evidence for 'megafloods' in arid subtropical Western Australia
1031 during the Little Ice Age Chronozone. Quaternary Science Reviews 144:107 – 122

1032 Sachse D, Billault I, Bowen GJ, Chikaraishi Y, Dawson TE, Feakins SJ, Freeman KH, Magill CR,
1033 McInerney FA, van dM, Marcel T.J., Polissar P, Robins RJ, Sachs JP, Schmidt H-L, Sessions AL,
1034 White JWC, West JB, Kahmen A (2012) Molecular Paleohydrology: Interpreting the
1035 Hydrogen-Isotopic Composition of Lipid Biomarkers from Photosynthesizing Organisms.
1036 Annual Review of Earth and Planetary Sciences 40:221–249

1037 Sachse D, Sachs JP (2008) Inverse relationship between D/H fractionation in cyanobacterial lipids
1038 and salinity in Christmas Island saline ponds. Geochimica et Cosmochimica Acta 72:793–806

1039 Sage RF, Christin P-A, Edwards EJ (2011) The C4 plant lineages of planet Earth. Journal of
1040 Experimental Botany 62:3155–3169

1041 Schmidt MWI, Torn MS, Abiven S, Dittmar T, Guggenberger G, Janssens IA, Kleber M, Kögel-
1042 Knabner I, Lehmann J, Manning DAC, others (2011) Persistence of soil organic matter as an
1043 ecosystem property. Nature 478:49–56

1044 Schouten S, Klein B, Wim, Blokker P, Schogt N, Rijpstra WIC, Grice K, Baas M, Sinninghe D, Jaap S
1045 (1998) Biosynthetic effects on the stable carbon isotopic compositions of algal lipids:
1046 Implications for deciphering the carbon isotopic biomarker record. Geochimica et
1047 Cosmochimica Acta 62:1397–1406

1048 Schulze ED, Nicolle D, Boerner A, Lauerer M, Aas G, Schulze I (2014) Stable carbon and nitrogen
1049 isotope ratios of *Eucalyptus* and *Acacia* species along a seasonal rainfall gradient in Western
1050 Australia. Trees 28:1125–1135

1051 Schwinning S, Sala OE, Loik ME, Ehleringer JR (2004) Thresholds, memory, and seasonality:
1052 understanding pulse dynamics in arid/semi-arid ecosystems. Oecologia 141:191–193

1053 Seki O, Nakatsuka T, Shibata H, Kawamura K (2010) A compound-specific *n*-alkane δ^{13}C and δD
1054 approach for assessing source and delivery processes of terrestrial organic matter within a
1055 forested watershed in northern Japan. Geochimica et Cosmochimica Acta 74:599–613

1056 Shepherd T, Wynne G, D (2006) The effects of stress on plant cuticular waxes. New Phytologist
1057 171:469–499

1058 Shi G, Cai W, Cowan T, Ribbe J, Rotstayn L, Dix M (2008) Variability and trend of North West
1059 Australia rainfall: observations and coupled climate modeling. Journal of Climate 21:2938–
1060 2959

1061 Shulmeister J, Lees BG (1995) Pollen evidence from tropical Australia for the onset of an ENSO-
1062 dominated climate at c. 4000 BP. The Holocene 5:10–18

1063 Skrzypek G (2013) Normalization procedures and reference material selection in stable HCNOS
1064 isotope analyses: an overview. Analytical and bioanalytical chemistry 405:2815–2823

1065 Skrzypek G, Dogramaci S, Grierson PF (2013) Geochemical and hydrological processes controlling
1066 groundwater salinity of a large inland wetland of northwest Australia. Chemical Geology
1067 357:164–177

1068 Snyder KA, Tartowski SL (2006) Multi-scale temporal variation in water availability: implications for
1069 vegetation dynamics in arid and semi-arid ecosystems. Journal of Arid Environments 65:219–
1070 234

1071 Sponseller RA, Heffernan JB, Fisher SG (2013) On the multiple ecological roles of water in river
1072 networks. Ecosphere 4:17, 1–14

1073 Stager JC, Ryves DB, King C, Madson J, Hazzard M, Neumann FH, Maud R (2013) Late Holocene
1074 precipitation variability in the summer rainfall region of South Africa. Quaternary Science
1075 Reviews 67:105–120

1076 Sun Q, Xie M, Shi L, Zhang Z, Lin Y, Shang W, Wang K, Li W, Liu J, Chu G (2013) Alkanes, compound-
1077 specific carbon isotope measures and climate variation during the last millennium from
1078 varved sediments of Lake Xiaolongwan, northeast China. Journal of Paleolimnology 50:331–
1079 344

1080 Tanner BR, Uhle ME, Kelley JT, Mora CI (2007) C3/C4 variations in salt-marsh sediments: An
1081 application of compound specific isotopic analysis of lipid biomarkers to late Holocene
1082 paleoenvironmental research. Organic Geochemistry 38:474–484

1083 Tanner BR, Uhle ME, Mora CI, Kelley JT, Schuneman PJ, Lane CS, Allen ES (2010) Comparison of
1084 bulk and compound-specific $\delta^{13}C$ analyses and determination of carbon sources to salt marsh
1085 sediments using *n*-alkane distributions (Maine, USA). Estuarine, Coastal and Shelf Science
1086 86:283–291

1087 Tipple BJ, Pagani M (2010) A 35Myr North American leaf-wax compound-specific carbon and
1088 hydrogen isotope record: Implications for C4 grasslands and hydrologic cycle dynamics. Earth
1089 and Planetary Science Letters 299:250–262

1090 Tissot BP, Welte DH (1984) (eds) Petroleum formation and occurrence, 2nd Ed. Springer-Verlag,
1091 New York, NY

1092 Tulipani S, Grice K, Krull E, Greenwood P, Revill AT (2014) Salinity variations in the northern
1093 Coorong Lagoon, South Australia: Significant changes in the Ecosystem following human
1094 alteration to the natural water regime. Organic Geochemistry 75:74–86

1095 Turner NC, Schulze E-D, Nicolle D, Schumacher J, Kuhlmann I (2008) Annual rainfall does not
1096 directly determine the carbon isotope ratio of leaves of Eucalyptus species. Physiologia
1097 Plantarum 132:440–445

1098 Unger IM, Motavalli PP, Muzika RM (2009) Changes in soil chemical properties with flooding: A
1099 field laboratory approach. Agriculture, Ecosystems & Environment 131:105–110

1100 van der Kaars S, De Deckker P, Gingele FX (2006) A 100 000-year record of annual and seasonal
1101 rainfall and temperature for northwestern Australia based on a pollen record obtained
1102 offshore. Journal of Quaternary Science 21:879–889

1103 van Etten EJB (2009) Inter-annual Rainfall Variability of Arid Australia: greater than elsewhere?
1104 Australian Geographer 40:109–120

van Soelen EE, Wagner-Cremer F, Damste JS, Reichart GJ (2013) Reconstructing tropical cyclone frequency using hydrogen isotope ratios of sedimentary *n*-alkanes in northern Queensland, Australia. Palaeogeography, Palaeoclimatology, Palaeoecology 376:66–72

Verschuren D (1999) Sedimentation controls on the preservation and time resolution of climate-proxy records from shallow fluctuating lakes. Quaternary Science Reviews 18:821–837

Vogts A, Moossen H, Rommerskirchen F, Rullkötter J (2009) Distribution patterns and stable carbon isotopic composition of alkanes and alkan-1-ols from plant waxes of African rain forest and savanna C3 species. Organic Geochemistry 40:1037–1054

Volkman JK, Barrett SM, Blackburn SI, Mansour MP, Sikes EL, Gelin F (1998) Microalgal biomarkers: a review of recent research developments. Organic Geochemistry 29:1163–1179

Volkman JK, Revill AT, Bonham PI, Clementson LA (2007) Sources of organic matter in sediments from the Ord River in tropical northern Australia. Organic Geochemistry 38:1039–1060

Voznesenskaya EV, Akhani H, Koteyeva NK, Chuong SDX, Roalson EH, Kiirats O, Franceschi VR, Edwards GE (2008) Structural, biochemical, and physiological characterization of photosynthesis in two C_4 subspecies of *Tecticornia indica* and the C_3 species *Tecticornia pergranulata* (Chenopodiaceae). Journal of Experimental Botany 59:1715–1734

Weiguo L, Xiahong F, Youfeng N, Qingle Z, Yunning C, Zhisheng AN (2005) $\delta^{13}C$ variation of C3 and C4 plants across an Asian monsoon rainfall gradient in arid northwestern China. Global Change Biology 11:1094–1100

Wolff C, Haug GH, Timmermann A, Damsté JSS, Brauer A, Sigman DM, Cane MA, Verschuren D (2011) Reduced interannual rainfall variability in East Africa during the last ice age. Science 333:743–747

1127 Zhou Y, Grice K, Stuart-Williams H, Farquhar GD, Hocart CH, Lu H, Liu W (2010) Biosynthetic origin
1128 of the saw-toothed profile in $\delta^{13}C$ and $\delta^{2}H$ of *n*-alkanes and systematic isotopic differences
1129 between *n*-, *iso*-and *anteiso*-alkanes in leaf waxes of land plants. Phytochemistry 71:388–403

1130 Zhou Y, Grice K, Chikaraishi Y, Stuart-Williams H, Farquhar GD, Ohkouchi N (2011) Temperature
1131 effect on leaf water deuterium enrichment and isotopic fractionation during leaf lipid
1132 biosynthesis: Results from controlled growth of C_3 and C_4 land plants. Phytochemistry
1133 72:207–213

1134

SUPPLEMENTARY MATERIAL

Table S1: Carbon stable isotopic distributions of *n*-alkanes (*n*-C) for sediments from P1– P3 of the 14 Mile Pool record

n-C	P1		P2		P3	
number	$\delta^{13}C$	Std	$\delta^{13}C$	Std	$\delta^{13}C$	Std
17	−32.3	0.1	-	-	-	-
18	-		-	-	-	-
19	−31.3	1.1	-	-	−29.5	0.1
20	−30.7	0.2	−27.9	0.4	−30.0	0.4
21	−30.9	0.3	−28.4	0.5	−30.1	0.9
22	−29.8	0.2	−27.2	0.3	−30.0	0.7
23	−29.5	0.2	−27.8	0.1	−29.5	0.1
24	−30.1	0.1	−28.4	0.3	−30.1	0.3
25	−29.6	0.0	−28.1	0.2	−29.5	0.1
26	−29.7	0.1	−29.4	0.1	−29.7	0.2
27	−29.3	0.0	−28.8	0.05	−28.4	0.2
28	−29.6	0.1	−29.7	0.3	−29.7	0.3
29	−29.8	0.1	−29.0	0.1	−28.6	0.1
30	−29.5	0.2	−29.3	0.1	−29.5	0.1
31	−30.2	0.1	−29.5	0.1	−28.4	0.1
32	−30.7	0.1	−29.6	0.3	−29.9	0.2
33	−29.7	0.1	−28.9	0.1	−27.5	0.2
34	−29.7	0.4	-	-	−27.8	0.3
35	−26.6	0.3	−25.8	0.1	−24.0	0.1

(1-COLUMN FITTING TABLE)

1142 **Table S2**: Compilation of foliar $\delta^{13}C$ values (Fig. 6) from C_3 woody plants collected from the non-

1143 riparian and riparian zone by the Ecosystems Research Group at The University of Western

1144 Australia over the 1997–2013 period in the semi-arid Pilbara region.

1145

Species	Location	Collection date	n	$\delta^{13}C$ [‰VPDB]	Std
Non-Riparian					
Acacia aneura	Red Hill	01-11-1997	2	−25.6	0.49
A. aneura	Floodplain	01-11-1997	2	−25.5	0.11
A. aneura sens. lat.	Flat Rocks, Yandicoogina	17–23-05-2004	12	−26.9	0.77
A. aneura sens. lat.	Paraburdoo	17–23-05-2004	24	−26.4	1.23
A. aneura sens. lat.	West Angelas	01-08-2007	12	−27.5	0.48
A. aneura sens. lat.	West Angelas	01-08-2007	5	−27.4	0.42
A. aneura sens. lat.	West Angelas	01-08-2007	4	−27.5	1.01
A. aneura sens. lat.	West Angelas	01-08-2007	10	−28.2	0.89
A. aneura sens. lat.	West Angelas	01-08-2007	13	−27.6	0.91
A. aneura sens. lat.	West Angelas	01-08-2007	13	−28.2	0.64
A. catenulata	West Angelas	01-08-2007	1	−28.9	-
A. catenulata	West Angelas	01-08-2007	11	−28.8	0.62
A. catenulata	West Angelas	01-08-2007	6	−27.8	0.47
A. catenulata	West Angelas	01-08-2007	6	−27.4	0.60
A. citrinoviridis	Barnett Ck	01-11-1997	2	−26.9	0.85
A. xiphophylla	Floodplain	01-11-1997	2	−26.8	0.53
A. xiphophylla	Red Hill	01-11-1997	2	−26.2	0.04
Callitris columellaris	Callitris Juna Downs	01-05-2003	61	−26.9	0.82
C. columellaris	Callitris Juna Downs	01-05-2004	108	−27.3	0.76
Riparian					
Eucalyptus camaldulensis	Marillana Ck Snooker	17-04-2011	5	−29.9	0.98
E. camaldulensis	Yule River control	11-11-2010	3	−31.2	0.57
E. leucophloia	Red Hill	01-11-1997	2	−25.5	0.27
E. victrix	Barnett Ck	01-11-1997	2	−28.7	0.20
E. victrix	Marillana Ck Snooker/control	17-04-2011	5	−30.6	0.90
E. camaldulensis/E. victrix	Yule River control	28-04-2011	5	−31.5	0.44
E. camaldulensis/E. victrix	Weeli Wolli Ck	02-02-2012	24	−30.9	1.24
E. camaldulensis/E. victrix	Weeli Wolli Ck	16-05-2012	21	−31.9	0.93
E. camaldulensis/E. victrix	Weeli Wolli Ck	21-08-2012	10	−31.8	1.09
E. camaldulensis/E. victrix	Weeli Wolli Ck	16-11-2012	20	−31.6	0.99
E. camaldulensis/E. victrix	Weeli Wolli Ck	27-03-2013	47	−31.8	0.98
Eucalyptus spp.	Ratty Springs, Pirraburdoo Ck	24-11-2005	9	−27.4	0.24
Melaleuca argentea	Marillana Ck	15-04-2001	20	−30.2	1.37
M. argentea	Marillana Ck Snooker/control	29-11-2009	5	−31.6	0.52
M. argentea	Marillana Ck Snooker/control	24-07-2010	5	−32.0	0.55
M. argentea	Marillana Ck Snooker/control	17-04-2011	5	−31.6	0.78
M. argentea	Weeli Wolli Ck	15-04-2001	20	−30.7	0.43
M. argentea	Yule River control	01-03-2009	5	−32.1	0.85
M. argentea	Yule River control	01-06-2009	5	−33.5	0.31
M. argentea	Yule River control	01-11-2009	5	−32.9	0.69
M. argentea	Yule River control	13-05-2010	5	−33.1	0.76
M. argentea	Yule River control	11-11-2010	3	−32.7	0.55
M. argentea	Yule River control	28-04-2011	5	−33.4	0.59
M. argentea	Marillana Creek	2001	10	−30.3	1.05
M. argentea	Weeli Wolli Ck	2001	10	−30.7	0.32

1146

1147 (1.5-COLUMN FITTING TABLE)